Hydraulic Fracturing Design and Optimization for Shale Oil Reservoir

by

Kan Wai Choong

12601

Bachelor of Engineering (Hons)

Petroleum Engineering

MAY 2013

Supervised by

Mohammad Amin Shoushtari

Universiti Teknologi PETRONAS

Bandar Seri Iskandar

31750 Tronoh

Perak

CERTIFICATION OF APPROVAL

Hydraulic Fracturing Design and Optimization for Shale Oil Reservoir

By

Kan Wai Choong (12601)

Dissertation submitted to the
Geoscience and Petroleum Engineering Department
Universiti Teknologi PETRONAS
in partial fulfillment of the requirement for the
BACHELOR OF ENGINEERING (Hons)
(PETROLEUM ENGINEERING)
for May 2013

Approved by,

_____

Mohammad Amin Shoushtari,
Supervisor,
Geoscience and Petroleum Engineering Department,
Universiti Teknologi PETRONAS.

Universiti Teknologi PETRONAS
Bandar Seri Iskandar
31750 Tronoh
Perak

CERTIFICATION OF ORIGINALITY

This is to certify that I, **KAN WAI CHOONG (12601, PETROLEUM ENGINEERING)**, is responsible for the work submitted in this project, that the work is original except specified in the references and acknowledgements, and herein have not undertaken or done by unspecified sources or persons.

This report is submitted to Universiti Teknologi PETRONAS for evaluation and safekeeping.

By,

_____

Kan Wai Choong,
12601,
Petroleum Engineering,
Universiti Teknologi PETRONAS.

Universiti Teknologi PETRONAS
Bandar Seri Iskandar
31750 Tronoh
Perak

ACKNOWLEDGEMENT

First and foremost, I would like to express my utmost gratitude to Mohammad Amin Shoushtari, my project Supervisor for his guidance and support. His patience and willingness to share knowledge regarding this topic has granted me the opportunity to seek knowledge, enhance my learning curve, and conduct and complete this project within the allocated time and in fulfillment of my degree requirement. The discussions I had with him were insightful, his constructive feedbacks and his dedication has always pushed me to strive for excellence. I would also like to extend my appreciation to Universiti Teknologi PETRONAS, Malaysia for providing me with the platform to improve my research skills and further prepare me to face the real world in the near future with this project course. My gratitude also goes to the Society of Petroleum Engineers-UTP-Student Chapter for funding my participation in the Paper Contest for the SPE Future Petroleum Engineers Conference 2013 in Beijing, China.

My ‘thank you’ to my friends for reminding me of the deadlines and for their constructive comments during my presentation practices. To Cha Yee Weng for being helpful throughout this project and to Manoj Matthew for his assistance on shale data, I thank you.

Special gratitude and appreciation to my family for their continuous support in all ways: emotional, spiritual, intellectual, physical and financial, through this project. With their kind nurture, I am grateful to be able to complete this project, at the same time experience this memorable journey of my Undergraduate study.

ABSTRACT

Shale oil reservoir, one of the unconventional-type reservoirs, is fast gaining attention worldwide. The reservoir has very low permeability but may produce liquid hydrocarbons and hydraulic fracturing is the completion technique usually applied. It is challenging to study hydraulic fracturing for shale oil reservoirs due to variations in reservoir and fluid properties. There is no general treatment to be employed. Hence, fracturing treatment is unique and exclusive where proper analysis is required for successful stimulation.

This 28-week project involves the 2-dimensional Perkins-Kern-Nordgren, PKN and Geertsma-de Klerk, GDK hydraulic fracturing models to obtain fracture geometry based on reservoir rock and fluid properties, and fracturing treatment data, while the Unified Fracture Design, UFD is used to calculate dimensionless productivity index, proppant number, dimensionless fracture conductivity, and optimized fracture geometry. The ultimate goal of this project is to develop a workflow based on the aforementioned models in Microsoft Excel that involves two parts: optimization study and design study. Identification of hydraulic fracturing parameters allows sensitivity studies to be performed for shale oil reservoir. Hypothetical cases have been designed. It is found that variations in parameters time, fracture height, injection rate, proppant pack permeability and reservoir permeability influence the optimization and parameters proppant mass, drainage area side length, proppant specific gravity, proppant porosity, plane strain modulus, viscosity and fracture height affects the design of hydraulic fracturing for shale oil reservoir, seen through illustrations of the results in graphs and tables. Thus, it is crucial to identify accurate and actual parameters to properly estimate fracture geometry or determine required treatment design for optimization.

The success of this project will heighten the knowledge and contribute to further research development on hydraulic fracturing design and optimization for shale oil reservoirs.

TABLE OF CONTENTS

LIST OF FIGURES

LIST OF TABLES

NOMENCLATURE

API	American Petroleum Institute
B	Oil formation volume factor
bopd	barrels of oil per day
C_{fD}	dimensionless fracture conductivity
$C_{fD,\ opt}$	optimized dimensionless fracture conductivity
C_L	leakoff coefficient ($ft/min^{1/2}$)
E’	plane strain modulus (psi)
h_f	fracture height (ft)
h_n	net height (ft)
I_x	penetration ratio
J_D	dimensionless productivity
k	reservoir permeability (md)
k_f	proppant pack permeability (md)
L_f	fracture half length (ft)
$L_{f,opt}$	optimized fracture half length (ft)
md	millidarcies
M_p	proppant mass (lbm)
N_p	proppant number
P_{net}	net pressure (psi)
q_i	injection rate (bbl/min)
$q_{i,opt}$	injection rate for optimized (bbl/min)
R	fracture radius (ft)
t_d	dimensionless time
t	time (min)
t_{opt}	time for optimized (min)
V_p	proppant bulk volume in net pay (ft^3)
V_r	drained reservoir volume (ft^3)
w_{max}	maximum fracture width (in)
w_w	fracture width at the wellbore (in)

$w_{w,opt}$	optimized fracture width at the wellbore (in)
$\bar{w}$	average fracture width (in)
x	distance from the wellbore (ft)
x_e	drainage area side length (ft)
x_f	fracture half length (ft)
y_e	breadth of single fracture drainage area (ft)
y_{eD}	aspect ratio
μ	viscosity (cp)
ρ_p	proppant material density (lbm/ft^3)
φ_p	proppant porosity

CHAPTER 1

INTRODUCTION

1.1 Background

Studies on unconventional reservoirs have emerged over the past few years and the industry continues to expand. New unconventional plays are reported every year. Unconventional reservoirs include shale oil, shale gas, tight gas sand, coal bed methane and heavy oil, and they refer to formations that cannot be produced economically without performing stimulation treatments or special recovery processes and technologies [1]. Shale oil reservoir is the focus of this project. Shale reservoirs can be referred to as reservoirs of extremely low permeability with hydrocarbon-bearing potential. Some popular shale oil plays in the US include the Bakken Shale, Eagle Ford Shale, Penn Shale, Utica Shale and Avalon Shale; and possible major shale oil plays in Vaca Muerta, Argentina; Bazhenov Shale, Russia; in China's Changqing field, Santanghu Basin, and Ordos Basin; Eastern Europe and Australia [2], [3]. The marginal cost to develop shale oil in the US is around USD 90 per barrel [3]

Hydraulic fracturing is one of the stimulation treatments for shale oil reservoirs. The general concept of hydraulic fracturing is to create a crack in the formation which leads to forming a fracture that eases the flow of oil and gas through the formation into the well using specially designed fracturing fluid under pressure. Two primary technologies have contributed to shale reservoir development; they are successful combination of multistage fracturing and horizontal wells [4]. The success of greater horizontal drilling activity and an increasing number of hydraulic fracture stages per lateral can be seen through North Dakota's Bakken shale play where its oil production grew six times, from 100,000 bopd to 600,000 bopd in seven years [5].

One of the issues related to hydraulic fracturing is the immense water consumption. To address water issue, some alternatives include using recycled water (treating flowback water), produced water (treated), formation water (water source wells) or sea water [6].

1.2 Problem Statement

There are available models to simulate hydraulic fracturing procedure but are limited in literature for shale oil reservoir study. The success of a hydraulic fracturing treatment is unique to the shale oil reservoir, where the completion program of one reservoir may not yield the same positive results when applied in other reservoirs. As reservoir properties vary significantly, this imposes additional challenges for the optimum treatment design [6]. Some reservoir properties are formation permeability, formation porosity, reservoir pressure, saturation, Poisson's ratio, and density profiles.

Fracture design treatment specifications like fracture height, width and length, fracturing fluid and proppant properties are also vital for treatment design as [7] there are no general or universal completion or stimulation design for shale oil wells. Proper and thorough analysis with the aid of models should be conducted. These parameters influence hydraulic fracturing design and its success, and hence press the need to select the optimum fracture treatment design when studying the shale oil reservoir.

1.3 Objectives of Study

The objectives of this study include:

- To develop a workflow for hydraulic fracturing simulation based on the PKN and GDK models and UFD for shale oil reservoirs, and compare and contrast the two hydraulic fracturing models;
- To analyze shale oil reservoir and fluid properties, and perform sensitivity studies on parameters related to optimization of hydraulic fracturing for shale oil reservoirs; and
- To determine design treatments required to achieve optimized fracture geometry and conduct sensitivity studies for shale oil reservoirs.

1.4 Scope of Study

The step-by-step scope of this study is:

- To understand and summarize the theoretical concepts of hydraulic fracturing, its terminology and available models;
- To review the two common PKN and GDK hydraulic fracturing models;
- To study the Unified Fracture Design;
- To learn about shale oil reservoir and its current hydraulic fracturing application;
- To identify the parameters involved in hydraulic fracturing treatment;
- To produce spreadsheet which includes PKN and GDK models and UFD;
- To analyze simulation results for optimization study that includes comparison of PKN and GDK models' fracture geometry estimation and dimensionless productivity index, and the sensitivity of each parameter;
- To analyze simulation results for design study that includes comparison of PKN and GDK models for required injection rate and time, and the sensitivity of each parameter; and
- To present quantitative results of sensitivity studies for optimization and design studies in graphs or tables.

1.5 Relevancy and Feasibility of Project

This project is relevant as to the Petroleum Engineering course and it is of current and popular topic to date. This project on hydraulic fracturing design and optimization for shale oil reservoir is feasible and within the time frame. Hypothetical case models are built and simulations for sensitivity studies are performed. Microsoft Excel is readily available as main tool of project.

CHAPTER 2

LITERATURE REVIEW

2.1 Hydraulic Fracturing in Shale Reservoirs

The earliest fracturing treatment was performed in the Hugoton gas field on July 1947 as it had low deliverability. Since then, the technology associated with hydraulic fracturing evolved and is constantly improving, increasing its applications and expanding its treatment onto challenging reservoirs. In general, hydraulic fracturing treatment in high permeability reservoirs will increase early life producing rates and accelerate productivity while in low permeability reservoirs, the ultimate recovery is increased instead [8].

Hydraulic fracturing is the process where the hydraulic pressure of fluid creates an artificial fracture in a reservoir and subsequently, this fracture grows in length, height and width due to the pumping mixture of hydraulic fluid and propping agents at high pressure into the wellbore. The energy applied to the crack tip must exceed the in-situ stress plus the tensile strength of the rock to create the fracture [9]. The fracturing fluid is used to create fracture and transport propping agents, or proppants, along the fracture. The function of proppants is to keep the fracture open. The fracturing fluids are designed to breakdown after fracturing job is completed so that the fluid can easily be removed. The penetrating fractures help to increase flow and drainage area in formations with low permeability, in compliance to King [10] where mentioned the intent of shale fracturing is to establish a higher permeability flow path from large sections of the reservoir to the wellbore. Generally, the aim of hydraulic fracturing is to design a fracture where fracture geometry stays within pay zone, thus developing the

maximum pay or producing formation contact and ultimately achieve maximum flow of hydrocarbons and minimize water production [10].

A fracture growth orientation is usually perpendicular to the plane of the least principle stress. These fractures usually grow until they are in contact with rocks of different structure, texture or strength to stop the fracture [10]. Another inhibiting mechanism for fracture growth and propagation is fracture fluid loss. As the fracture contact area with the formation increases or when the fluid invades natural fractures in the formation, part of the fracturing fluid is lost into the formation, hence decreases the amount of fracturing fluids remaining to propagate fracture into formation [8].

Shale is a fine-grained sedimentary rock formed by consolidation and compaction of clay and silt sized particles into thin, relatively extremely low permeable layers, commonly known as mud. These rocks have relatively large amounts of organic matter known as kerogen and have potential to become rich hydrocarbon source rocks. It has often been confusing between shale oil and oil shale resources. The heating of rocks that contain kerogen to as high as 950 degrees Fahrenheit, in a process called retortion, produce oil shale. This means that liquid oil is generated synthetically. In contrast, shale oil need not be heated over time for production. In other words, shale oil can be said as crude oil that is produced from tight shale formations.

Shale reservoirs are said to be very low permeability reservoirs with hydrocarbon-bearing potential. Conventional sandstones may have permeabilities in the range of 0.5 to 20 md while shale reservoirs may have permeabilities of 0.000001 to 0.0001 md. Recently the drive to locate and develop shale oil reservoirs has become rapid. Several shale oil plays such as the Bakken shale and the Eagle Ford shale show positive results from employing hydraulic fracturing stimulation technology on these unconventional reservoirs. The Eagle Ford Shale is a unique play with different reservoir fluids, from dry gas to black oil [11]. The light oil is estimated to be 41^{o} API while the rich condensate and lean condensate are estimated at 51^{o} to 52^{o} API and 50^{o} API respectively [12]. The typical North Dakota's Bakken property shows 42^{o} API [13]. As

this study focuses on shale oil reservoirs, the following findings compare shale oil to shale gas reservoirs, primarily on hydraulic fracturing treatment.

Drilling and completion of wells are similar to shale oil and gas reservoirs but hydraulic fracturing treatments are different depending on the fluid formation type. In fracturing fluid selection, slickwater fluid system is pumped for gas rich areas whereby hybrid or crosslink fluid system for the liquids-rich areas [11]. Larger diameter proppants, from small mesh proppants to 30/50 and 20/40 meshes, are needed in shale oil reservoirs as compared to shale gas reservoirs. Employment of crosslink fluids allow placement of moderate to larger mesh proppants and crosslinked fluids require only 30-50 % of the water needed in slickwater operations. Higher proppant concentrations and higher viscosity fluids are also needed in shale oil reservoirs as compared to shale gas reservoirs [4], [11], [14]. Generally, oil wells require more conductivity than gas wells as oil is less mobile than gas, and thus, multiphase oil production requires significantly greater fracture conductivity than single phase gas production [6]. A summary of the hydraulic fracturing treatments for shale oil reservoir is shown in Table 1.

Table 1- Summary of hydraulic fracturing treatments for shale oil reservoirs.

Source	Treatment
Ilk, DeGolyer, MacNaughton, Broussard & Blasingame (2012); Palisch, Chapman & Godwin (2012)	Hybrid or crosslink fluid
Palisch, Chapman & Godwin (2012); Pope, Palisch & Saldungaray (2012)	Larger diameter proppants, from small mesh to 30/50 or 20/40
Kennedy (2012)	Require more conductivity that gas well
Ilk, DeGolyer, MacNaughton, Broussard & Blasingame (2012); Palisch, Chapman & Godwin (2012); Pope, Palisch & Saldungaray (2012)	High proppant concentration and higher viscosity fluid

Another interesting point on the difference in formation fluid is the reservoir management aspect whereby condensate reservoirs have been challenging due to condensate blockage. Once the bottomhole pressure drops below the dew point, liquid or condensate drops out. Thus, variations in the PVT behaviour throughout the play area and near critical PVT behaviour become an important component of production performance [11].

2.2 Production from Shale Oil Reservoir

As discussed in the earlier section, the combination of hydraulic fracturing and horizontal drilling has shown to return positive results with an increase in oil production. However, about 90 to 95 percent of the Bakken and Three Forks shale oil resource are remained in the ground through these oil recovery methods. To improve recovery in the Bakken resource, enhanced recovery methods may need to be employed. This includes the possibility of using injection of carbon dioxide or raw shale gas underground so that pressure at subsurface increases to push oil through the dense rocks [15].

Another potential approach to producing shale oil is to employ waterflooding technique [15], [16]. By placing water underground, the water pushes oil into nearby producing wells and this method is cheap to try and run, about USD 5 to 10 per barrel. Pinecrest mentioned that they can increase the amount of oil recovered by two fold while Raging River projects that recovery factor increases to 16 to 20% from 8% [16].

On the bright side, although uncertain to how effective and affordable the advanced techniques will be for the Bakken shale (laboratory tests displayed promising findings at present), producing from a relatively small part of the large oil content resource in the Bakken field will impact the US oil production [15].

2.3 2-Dimensional Models

The use of 2-dimensional models to calculate fracture geometry during the fracture optimization process will save computer time and speed up calculation process [17]. There are several models in literature that gives reasonable approximations of induced fractures. 2-D models incorporated four basic principles: fluid flow, rock mechanics, continuity and fracture width. These models can be used when barriers are strong. Khristianovich and Zheltov, in 1955, developed a model that considers fracture mechanics with simple assumptions on fluid flow. In 1957, Carter built a model by focusing on fluid leakoff and ignored fluid viscosity effects and solid mechanics, while Perkins and Kern, in 1961, focused on fluid flow and neglected the role of fracture mechanics. Geertsma and de Klerk, in 1969, included fluid loss and developed the work by Khristianovich and Zheltov to produce the now known as GDK model. In 1972, Nordgren added leakoff and storage width to Perkin and Kern's model, developing the PKN model [1]. This section will describe the differences between the two most popular hydraulic fracturing models, the mutually exclusive PKN and GDK models, and a brief analysis on the models to be used in this shale oil reservoir project.

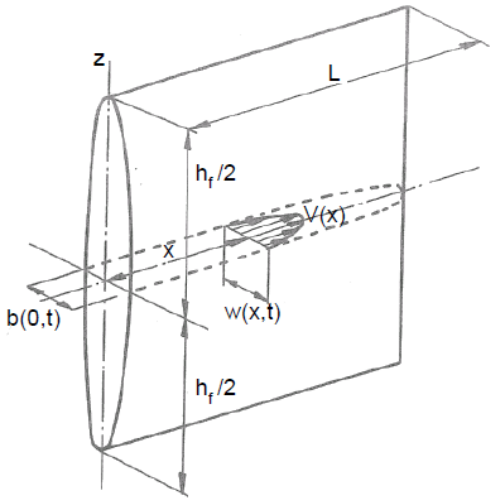

Figure 1- PKN fracture model [1].

The PKN geometry model approximates the geometry as an elliptical shape in both the vertical and horizontal axes (Figure 1) with constant height fracture and does not exceed pay zone. In both directions, the width is smaller than the other dimensions. This model

is most applicable for fractures with length to half height ratios greater than one. The Perkins and Kern model assumes that every vertical cross section acts independently and the pressure at a section is dominated more by the height of the section than by the length of the fracture. At any cross section, the maximum width is proportional to the net pressure at that point and independent of the width at any other point. The fracture width at any point is proportional to its height. Nordgren considered leakoff and storage width, and defined a dimensionless time term for two cases: storage dominated or high efficiency where t_d is less than 0.01, and high leakoff for t_d more than 1 to identify which one of two to use to obtain the fracture length and width [1].

$$t_d = \left(\frac{64 C_L^5 E' h_f}{\pi^3 \mu q_i^2} \right)^{\frac{2}{3}} t . \quad \text{.....(2.1)}$$

Case 1: Storage dominated or high efficiency

$$L(t) = 0.39(t)^{\frac{4}{5}} (\frac{E' q_i^3}{h_f^4 \mu})^{\frac{1}{5}}; \quad \text{.....(2.2)}$$

$$w_w = 2.18(t)^{\frac{1}{5}} (\frac{q_i^2 \mu}{E' h_f})^{\frac{1}{5}}. \quad \text{.....(2.3)}$$

Case 2: High leakoff

$$L(t) = (t)^{\frac{1}{2}} (\frac{q_i}{2\pi h_f C_L});. \quad \text{.....(2.4)}$$

$$w_w = 4(t)^{\frac{1}{8}} (\frac{q_i^2 \mu}{\pi^3 E' C_L h_f})^{\frac{1}{4}} \quad \text{.....(2.5)}$$

For any point at a distance *x* from the wellbore, the following approximation for the PKN model is Equation 2.6.

$$w = w_{\max} \left[1 - \left(\frac{x}{L} \right) \right]^{\frac{1}{4}} \quad \text{.....(2.6)}$$

$$\overline{w} = \frac{\pi}{5} w_{\max} \quad \text{.....(2.7)}$$

Given

$$P_{net} = \left[\frac{16 \mu q_i E'^3 L}{\pi h_f^4} \right]^{\frac{1}{4}} \quad \text{.....(2.8)}$$

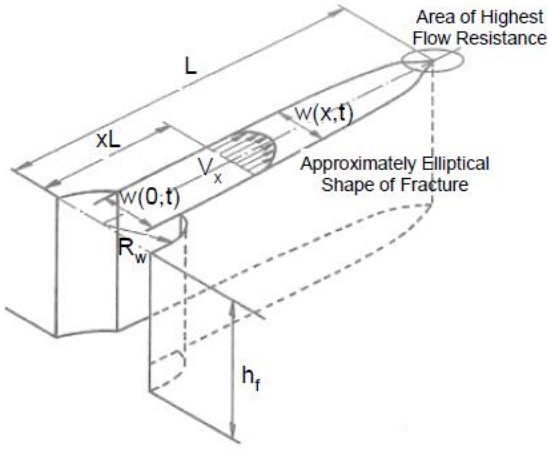

Figure 2- GDK fracture model [1].

The GDK geometry model also assumes a constant height fracture and does not exceed pay zone but with horizontal plane strain. The cross sectional area perpendicular to the direction of fracture propagation is rectangular in shape while it is elliptical in shape parallel to the fracture propagation (Figure 2). Other assumptions include slippage between layers, fluid does not act on entire fracture length and fracture width is constant along its height. This model is most applicable for fractures with length to half height ratios less than one. The length and width can be expressed as a function of time for two different cases, that is, for no leak-off and high leak-off cases [1].

Case 1: No leak-off

$$L(t) = 0.38(t)^{\frac{2}{3}} \left(\frac{E' q_i^3}{h_f^3 \mu} \right)^{\frac{1}{6}} \quad \text{.....(2.9)}$$

$$w_w = 1.48(t)^{\frac{1}{3}} \left(\frac{q_i^3 \mu}{E' h_f^3} \right)^{\frac{1}{6}} \quad \text{.....(2.10)}$$

Case 2: High leak-off

$$L(t) = t^{\frac{1}{2}}\left(\frac{q_i}{2\pi h_f C_L}\right) \quad \text{.....(2.11)}$$

For high leak-off, no explicit equation for width has been provided. Any point at a distance *x* from the wellbore is Equation 2.12.

$$w = w_{\max}\left[1-\left(\frac{x}{L}\right)\right]^{\frac{1}{2}} \quad \text{.....(2.12)}$$

$$\bar{w} = \frac{\pi}{4} w_{\max} \text{.....(2.13)}$$

where $w_{\max} = (\frac{8P_{net}R}{E'})$ .....(2.14)

and $P_{net,w} = \left(E'^3 \frac{21 q_i \mu}{64\pi h_f L^2}\right)^{\frac{1}{4}}$ .....(2.15)

Hence, one difference between the two lies in terms of its approach where the PKN model fracture cross section in the vertical plane, perpendicular to the long axis generally maintains an elliptical shape while the GDK model approximates elliptical shape in the horizontal plane and a rectangular shape vertically. The both also differ in terms of its applicability for the desired treatment in formations. The range of the fracture half length generated with the PKN model is almost twice that of GDK model while the range of fracture width generated for GDK model is approximately 50 percent more than the PKN model [1]. Thus, the GDK model normally predicts shorter fracture lengths than the PKN model but the GDK model predicts a wider fracture [17], [18]. Table 2 shows a summary of general description of the models based on the literature review.

Table 2- Summary of general description of PKN and GDK models from literature review.

Property	**Perkins-Kern-Nordgren Model (1972)**	**Geertsma- de Klerk Model (1969)**
Shape	Elliptical shape horizontally and vertically	Elliptical shape in the horizontal plane and rectangular shape vertically
Fracture half length	Predicts longer	Predicts shorter
Fracture width	Less wide	Wider
Assumptions	Neglects effects of fracture tip and fracture mechanics; focuses on fluid flow and their pressure gradients; height of vertical fracture is constant and does not exceed payzone; maximum width is proportional to net pressure at that point and independent of the width at any other point	Fracture width is proportional to its fracture length; fracture height is constant; there is slippage between layers; fluid does not act on entire fracture length; fracture width is constant along its height

This project focuses on comparing the PKN and GDK models for fracture geometry and later employed in optimization study.

2.4 Unified Fracture Design

After fracturing, a production analysis should be done to identify the optimum design and its treatment specifications. The productivity index represents the production rate well, and in oil wells, the dimensionless productivity, J_D can be used. The J_D is calculated as

$$J_D = \frac{141.2qB\mu}{kh\Delta p} \quad \text{.....(2.16)}$$

The Unified Fracture Design (UFD) is introduced by Economides and the proppant number, N_P is an important parameter for UFD.

$$N_p = \frac{C_{fD} I_x^2}{y_{eD}} \quad \text{.....(2.17)}$$

Where

$$I_x = \frac{2x_f}{x_e} \text{.....(2.18)}$$

$$C_{fD} = \frac{k_f w}{k x_f} \text{.....(2.19)}$$

$$y_{eD} = \frac{x_e}{y_e} \text{.....(2.20)}$$

Hence, the proppant number can be written as

$$N_p = \frac{4k_f x_f^2 w}{k x_f x_e^2} = \frac{2k_f}{k} \frac{2x_f w}{x_e^2} x \frac{h_n}{h_f} = \frac{2k_f V_p}{k V_r} \quad \text{.....(2.21)}$$

Or $$N_p = \frac{2k_f V_p}{k h x_e^2 y_{eD}} \text{.....(2.22)}$$

Where with reasonable approximation, proppant bulk volume is calculated as

$$V_p = \frac{M_p}{\rho_p (1-\varphi_p)} x \frac{h_n}{h_f} \text{.....(2.23)}$$

With proppant number determined, the maximum dimensionless productivity index can be found as the peak value of the appropriate curve corresponding to the known proppant number and the optimum dimensionless fracture conductivity read under the peak. Shown in Figure 3 is an example of the dimensionless productivity index against dimensionless fracture conductivity plot for various proppant numbers where drainage area side length equals the drainage area breath of single fracture [19].

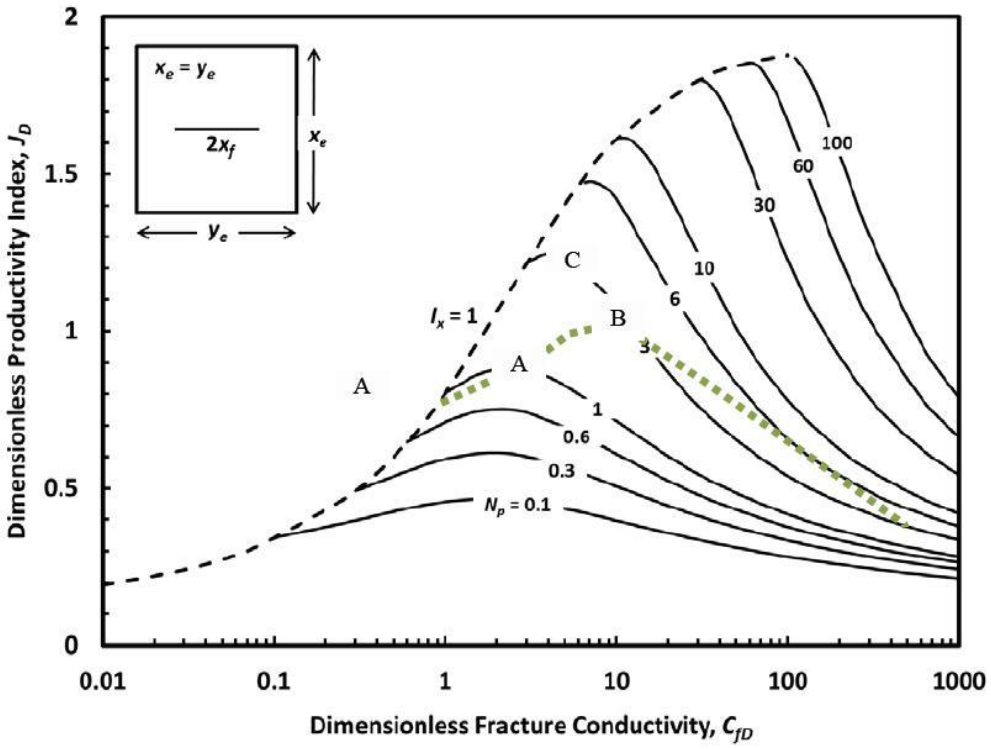

Figure 3- Dimensionless productivity index as a function of C_{fD} with curve parameter N_{prop} [16].

The optimum dimensionless fracture conductivity value is obtained where dimensionless productivity index is the maximum for the proppant number. For very low permeability reservoirs like shale oil reservoirs, the proppant number can be very high. An empirical calculation for dimensionless fracture conductivity and dimensionless productivity index as a function of aspect ratio and proppant number is developed by Bhattacharya, Nikolaou and Economides [20] shown in Equations 2.24 and 2.25.

$$C_{fD,opt} = 1.6\sqrt{\frac{\left(1+0.03N_p^2\right)\left(1+1.3N_p^2\left(y_{eD}^{-1.2}\right)\right)}{1+0.1N_p^2\left(y_{eD}^{-3.2}\right)}} \quad \text{.....(2.24)}$$

$$J_{D,\max} = \frac{0.6y_{eD}^{0.7} + 14y_{eD}^{1.6}N_p + 28y_{eD}^{2.7}N_p^2}{1+35y_{eD}^{1.75}N_p + 14y_{eD}^{3.7}N_p^2} \quad \text{.....(2.25)}$$

Alternatively, the optimum fracture half length and fracture width can be back-calculated if proppant number and data are known using Equations 2.26 and 2.27 [19], [20].

$$L_{opt} = \sqrt{\frac{k_f V_f}{C_{fD,opt} kh}} \quad \text{.....(2.26)}$$

$$w_{opt} = \sqrt{\frac{C_{fD,opt} k V_f}{k_f h}} \quad \text{.....(2.27)}$$

Where $V_f = \frac{V_p}{2}$ .....(2.28)

CHAPTER 3

METHODOLOGY

This simulation-based study is expected to provide valuable findings for hydraulic fracturing design and in shale oil reservoirs. The methodology is divided into two parts: forward for optimization by calculation of fracture geometry, and backward for determination of hydraulic fracturing design to achieve optimized fracture geometry, illustrated in Figure 4. The 'blue' arrow indicates general flow of the optimization study while the 'green' arrow indicates general flow of the design study.

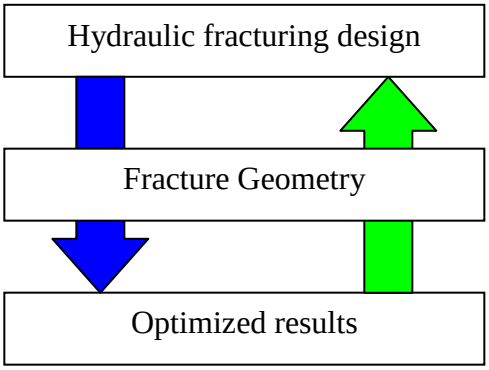

Figure 4- General description of the two studies.

3.1 Research Schedule

This 28-week project is generally divided into two phases, named: FYP 1 and FYP 2, and consists of 14 weeks each. The project began with the selection of topic. After acquiring the title of study, preliminary research work is started that included understanding the hydraulic fracturing concepts, learned about shale oil reservoirs, and analyzed the available models in literature for hydraulic fracturing (the PKN and GDK models) and Unified Fracture Design. Concurrently, this period comprised of

identification of the problem statement to address throughout this project, specifying the objectives of this project and the scope of work, writing literature review of current and relevant research papers and proposing methodology until submission of 'Extended Proposal' on Week 7. The 'Proposal Defence', an oral presentation to the supervisor and one internal examiner, was held. The project continued with obtaining of shale information and hydraulic fracturing treatment data (in literature or reports) and began developing the models, which are the PKN model and the Unified Fracture Design, on Microsoft Excel. After these have been successfully designed, preliminary studies using hypothetical cases were performed. These included design and optimization studies, and further investigation on effects of variations of parameters by running sensitivity studies until the submission of 'Interim Report' on Week 14 [21].

The second phase of the project covered the continuation of project until completion and documenting tasks. The project continued with the inclusion of the GDK model, comparison of models PKN and GDK on fracture geometry, completion of spreadsheet for base cases optimization study and design study, and parametric studies for further investigations. Several key milestones are achieved for the documenting duty. The 'Progress Report' is submitted on Week 8, technical paper is produced by Week 11, Pre-SEDEX is scheduled in Week 13, the, Oral Presentation is scheduled in Week 14 and finally, submission of dissertation of project is by Week 14 [21].

The Gantt charts for FYP 1 and FYP 2 phases are shown in Figures 5 and 6, with marked key milestones to denote important dates and events throughout this project.

No	Detail/ Week	1	2	3	4	5	6	7	8	9	10	11	12	13	14
1	Topic Selection														
2	Preliminary Research Work • Hydraulic fracturing • Shale oil reservoir • Models and J_D														
3	Extended Proposal							**							
4	Proposal Defense									**					
5	Project Work • Obtain data (shale, proppant) • Model building • Preliminary results • Sensitivity study														
6	Interim Report • Reporting • Submission														**

Key Milestone **

Figure 5- Gantt chart for the first phase of project.

No	Detail/ Week	1	2	3	4	5	6	7	8	9	10	11	12	13	14
1	Project Work														
	• Complete base cases for studies														
	• Comparison of models														
	• Parametric study														
2	Reporting, Documentation and Submission														
	• Progress Report								**						
	• Draft Paper											**			
	• Technical Paper											**			
	• Pre-SEDEX													**	
	• Oral Presentation														**
	• Dissertation (hard bound)														**

Key Milestone **

Figure 6- Gantt chart for the second phase of project.

3.2 Optimization Study

The PKN model, with cross sections an elliptic shape with maximum width in the centre, for vertical linear fracture propagation assumes the fracture height (independent of the fracture length), fracturing fluid pressure is constant in vertical cross section perpendicular to the direction of propagation, each vertical cross section deforms individually and not affected by its neighbours, and fluid pressure falls off towards the tip or leading edge [8]. The dimensionless time will be calculated using Equation 2.1 to identify which one of two cases is to be employed.

The GDK model has elliptical shape in the horizontal plane and rectangular shape vertically. The assumptions involved using GDK model is that fracture width is proportional to its fracture length, fracture height is constant, there is slippage between layers, fluid does not act on entire fracture length and fracture width is constant along its height [8]. All data required for this study is shown in Table 3. The blue boxes indicate data required for study, the yellow boxes indicate calculation in the Excel spreadsheet while the green boxes display results. In other words, the 'Calculation data' represents midway calculation steps that are used by 'Results' to arrive at the final output.

Table 3- Input data required and data calculated for optimization study.

Data	Value	Unit
Time		min
Fracture height		ft
Injection rate		bbl/min
Plane strain modulus		psi
Viscosity		cp
Leakoff coefficient		$ft/min^{1/2}$
Proppant pack permeability		md
Reservoir permeability		md
Drainage area side length		ft
Aspect ratio		-
Penetration ratio		-
Proppant number		-
Dimensionless fracture conductivity		-
Fracture half length		ft
Fracture width at wellbore		in
Dimensionless productivity index		-

Legend:
- Input data
- Calculation data
- Results

With these data, the PKN and GDK models calculate fracture geometry, particularly fracture half length and fracture width. These results will be needed to calculate the dimensionless productivity index. Proppant number, penetration ratio and dimensionless fracture conductivity are calculated from Equations 2.17, 2.18 and 2.19 respectively. The underlying assumption of this procedure is that the dimensionless fracture conductivity calculated is optimum for the calculated fracture geometry, the calculation of the dimensionless productivity index is similar to the maximum dimensionless productivity index using Equation 2.25, and for a single fracture, single well of square shape. A comparison on fracture geometry calculated between the PKN and GDK models is performed.

The dimensionless productivity index is plotted and the optimal design for the parameter is indicated by the highest or peak of the dimensionless productivity index graph. Following these steps, sensitivity studies are conducted for various cases to study its effects on optimization using both PKN and GDK models. Figure 7 illustrates the work flow diagram of this optimization study.

3.3 Design Study

The data required is shown in Table 4. Similarly in Legend to the ptimization study, the blue boxes indicate the input data required, the yellow boxes show calculation steps to arrive at the results, shown as green boxes.

Table 4- Input data required and data calculated for design study.

Data	Value	Unit
Proppant mass		lbm
Proppant density		lbm/ft^3
Proppant porosity		-
Formation height		ft
Proppant pack permeability		md
Reservoir permeability		md
Proppant to pay		%
Aspect ratio		-
Plane strain modulus		psi
Viscosity		cp
Leakoff coefficient		$ft/min^{1/2}$
Fracture height		ft
Proppant bulk volume		ft^3
Proppant number		-
Optimized dimensionless fracture conductivity		-
Optimized fracture half length		ft
Optimized fracture width		in
Time		min
Injection rate		bbl/min

Legend:
- Input data
- Calculation data
- Results

The dimensionless fracture conductivity, with usually very high proppant number for very low permeability reservoirs like shale oil reservoirs, is calculated using Equation 2.24 where proppant number is calculated from Equation 3.1. The corresponding optimum fracture half length and fracture width can be estimated from Equations 2.26 or 3.2, and 2.27 respectively.

$$Np = \frac{2k_f V_p}{khy_{eD}x_e^2} \quad \text{.....(3.1)}$$

. $$L_{f,opt} = \sqrt{\frac{k_f V_p}{2khC_{fD,opt}y_{eD}}} \quad \text{.....(3.2)}$$

From the optimized fracture half length and fracture width, the required time and injection rate to achieve these results can be solved simultaneously for the PKN or GDK model. For PKN model, the equations are simplified to Equations 3.3 and 3.4 for Case 1 of high efficiency and Equations 3.5 and 3.6 for Case 2 of high leak-off, assuming fracture height, plane strain modulus, viscosity, and leak-off coefficient are known and constant.

$$t_{opt} = \left(\frac{4.08 \mu^{\frac{1}{3}} L_{opt}^{\frac{2}{3}} h_f^{\frac{1}{3}}}{E'^{\frac{1}{3}} w_{opt}} \right)^3 \quad \text{.....(3.3)}$$

$$q_{i,opt} = \left(\frac{L_{opt}^5 \mu h_f^4}{0.009 t_{opt}^4 E'} \right)^{\frac{1}{3}} \quad \text{.....(3.4)}$$

$$t_{opt} = \frac{65536}{w_{opt}^8} \left(\frac{4 h_f C_L L_{opt}^2 \mu}{\pi E'} \right)^2 \quad \text{.....(3.5)}$$

$$q_{i,opt} = \frac{2 \pi h_f C_L L_{opt}}{\sqrt{t_{opt}}} \quad \text{.....(3.6)}$$

For GDK model, the time and injection rate equations are simplified to Equations 3.7 and 3.8 for Case 1 of no leak-off only, assuming fracture height, plane strain modulus, viscosity and leak-off coefficient are known and constant. Derivation of the time and injection rate for Case 2 of high leak-off is not made.

$$t_{opt} = \left(\frac{3.89 L_{opt} \mu^{\frac{1}{3}}}{w_{opt} E'^{\frac{1}{3}}} \right)^3 \quad \text{.....(3.7)}$$

$$q_{i,opt} = \left(\frac{L_{opt}^6 h_f^3 \mu}{0.003 t_{opt}^4 E'} \right)^{\frac{1}{3}} \quad \text{.....(3.8)}$$

In this project, based on preliminary study, only Case 1 for both models is applied during sensitivity studies. The Figure 8 illustrates the work flow diagram of this design study.

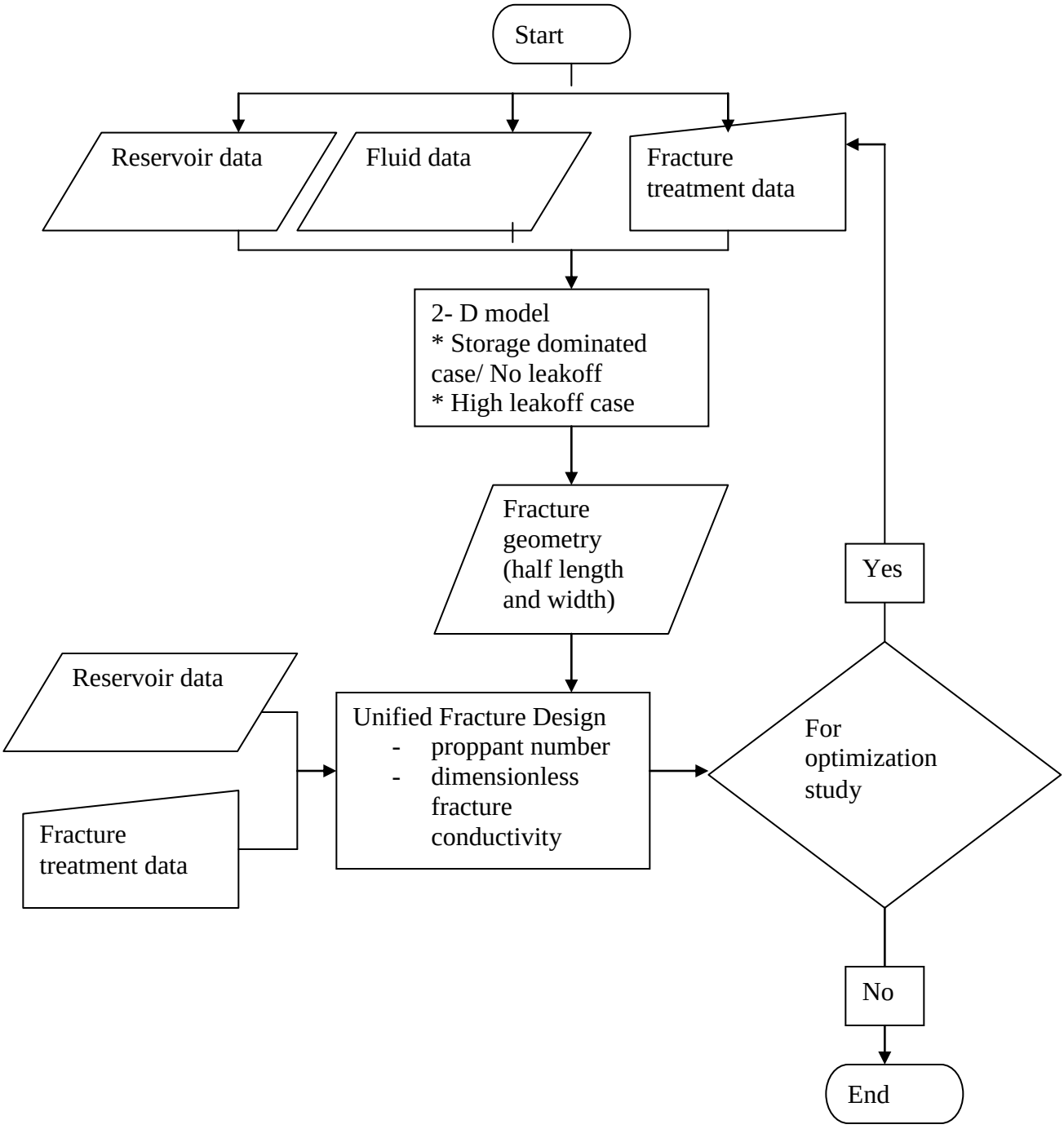

Figure 7- Flow diagram of optimization study.

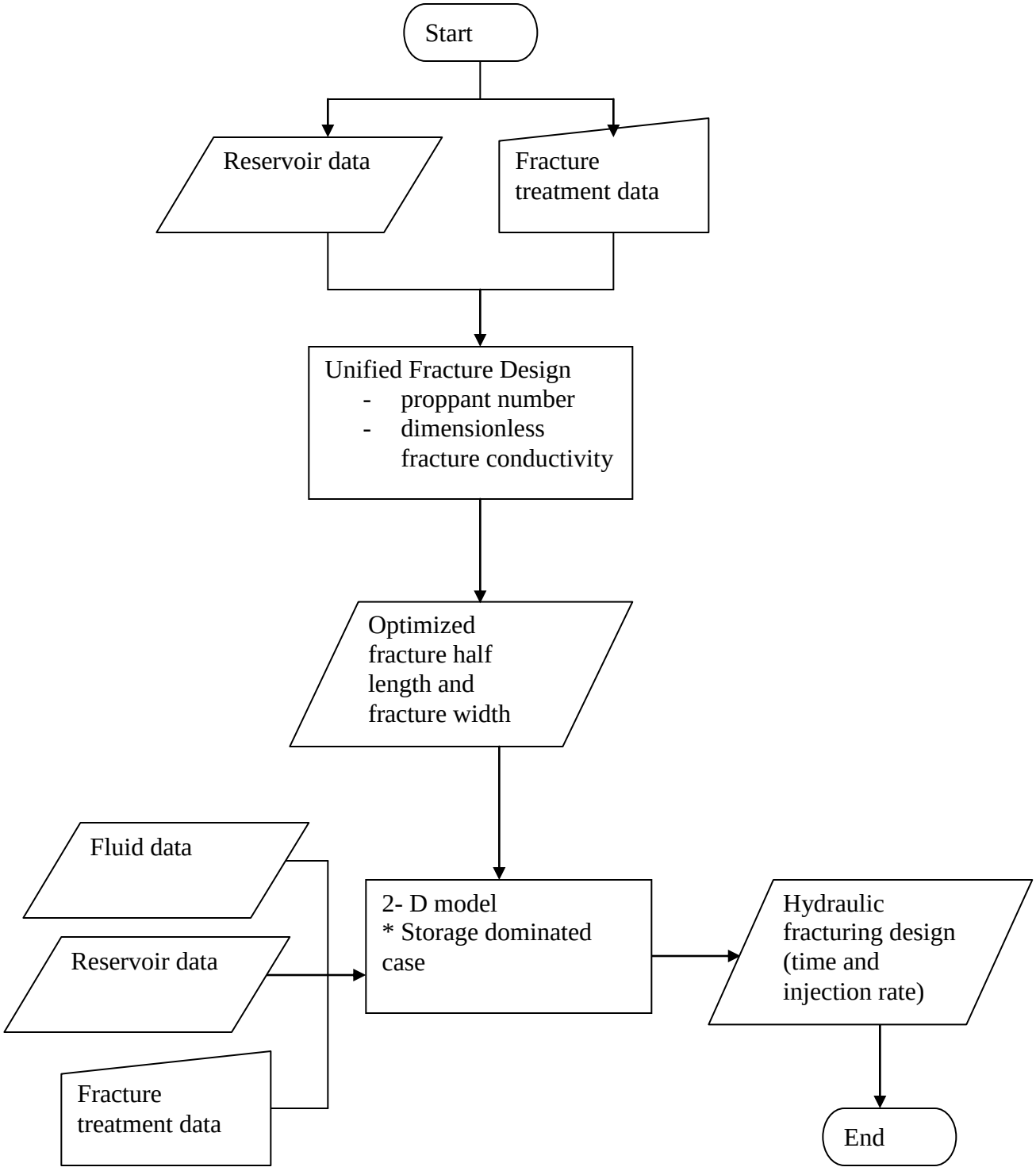

Figure 8- Flow diagram of design study.

3.4 Tools

The most important tool employed in this project is Microsoft Excel, where spreadsheets are designed for calculation. Snapshots of the Microsoft Excel spreadsheet are enclosed in Appendix A. Microsoft Office such as Microsoft Words, Microsoft Excel and Microsoft PowerPoint is used for collection or organization of results, reporting, documentation and presentation.

3.5 Hypothetical Case

To demonstrate the use of this methodology, for both optimization and design studies, one hypothetical base case each has been developed [20], as shown in Tables 5 and 6 respectively. Several sensitivity studies have been conducted to illustrate the effect of variation of parameters. In optimization study, 12 different values of parameters time, fracture height, injection rate, plane strain modulus and viscosity are selected for fracture geometry and dimensionless productivity index sensitivity studies, and 12 different values of parameters proppant pack permeability and reservoir permeability are also selected for dimensionless productivity index sensitivity study. For sensitivity analysis on design study, 5 different values of parameters proppant mass, reservoir permeability, drainage area side length, proppant specific gravity, proppant pack permeability, proppant porosity, fracture height (assuming fracture height is equal to formation height), plane strain modulus and viscosity, and 3 different values of aspect ratio are selected to illustrate the effect of parameter variation on time and injection rate required. The input values for parametric studies are enclosed in Appendix B.

Table 5- Hypothetical case input data for optimization study.

Data	**Value**	**Unit**
Time	600	min
Fracture height	60	ft
Injection rate	100	bbl/min
Plane strain modulus	3.00E+06	psi
Viscosity	200	cp
Leakoff coefficient	0.005	$ft/min^{1/2}$
Proppant pack permeability	3000	md
Reservoir permeability	0.0001	md
Drainage area side length	2000	ft

Table 6- Hypothetical case input data for design study.

Data	**Value**	**Unit**
Proppant mass	200000	lbm
Proppant specific gravity	2.65	-
Proppant density	165.36	Lbm/ft^3
Proppant porosity	0.35	-
Formation height	60	ft
Fracture height	60	ft
Proppant pack permeability	200000	md
Reservoir permeability	0.00005	md
Drainage area side length	2000	ft
Proppant to pay	100	%
Aspect ratio	1	-
Plane strain modulus	3.00E+06	psi
Viscosity	200	cp
Leakoff coefficient	0.005	$ft/min^{1/2}$

To illustrate the sensitivity of parameters in the studies, a set of parameters with values 50% more than the base case is designed. Equation 3.9 shows the calculation of percentage difference in result.

$$difference(\%) = \frac{\mathrm{Re}sult_{new} - \mathrm{Re}sult_{base}}{\mathrm{Re}sult_{base}} x100\% \quad \ldots\ldots\ldots\ldots\ldots\ldots\ldots\ldots\ldots\ldots\ldots\ldots (3.9)$$

CHAPTER 4

RESULTS AND DISCUSSIONS

As discussed in Methodology section, several hypothetical cases have been investigated. Following are the results and discussion based on the designed cases.

4.1 Optimization Study

4.1.1 Comparison between PKN and GDK Models on Fracture Geometry

Using the same input data for both PKN and GDK models, a comparison study between the two models on fracture geometry is performed. For both models, Case 1 high efficiency or no leak-off is applied as for shale oil reservoirs, where very small dimensionless time values are observed. Results for five parameters: time, fracture height, injection rate, plane strain modulus and viscosity, are presented for fracture half length in Figures 9 to 13 and fracture width at wellbore in Figures 14 to 18.

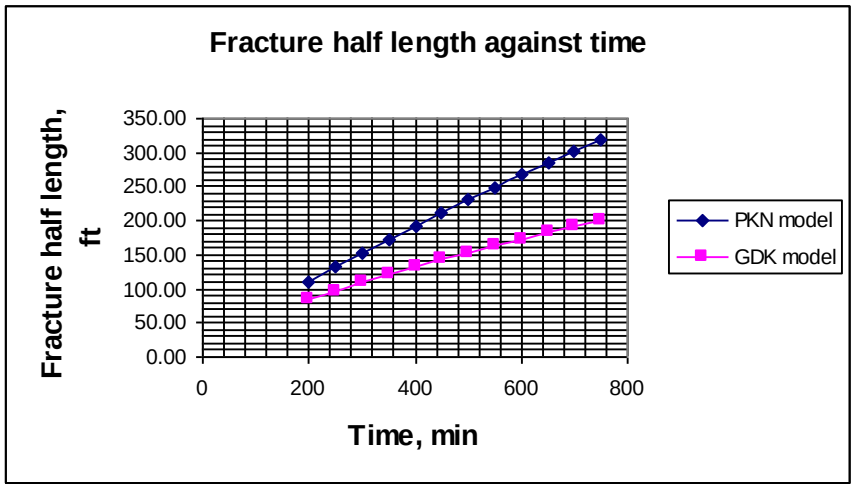

Figure 9- Comparison between PKN and GDK models for fracture half length on parameter time.

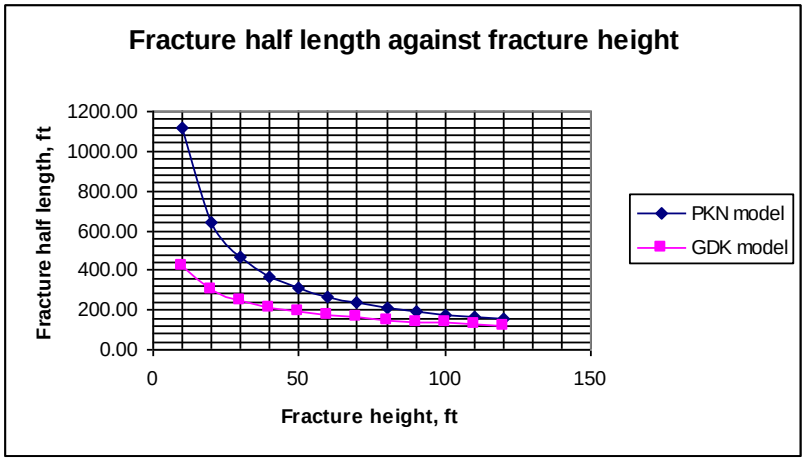

Figure 10- Comparison between PKN and GDK models for fracture half length on parameter fracture height.

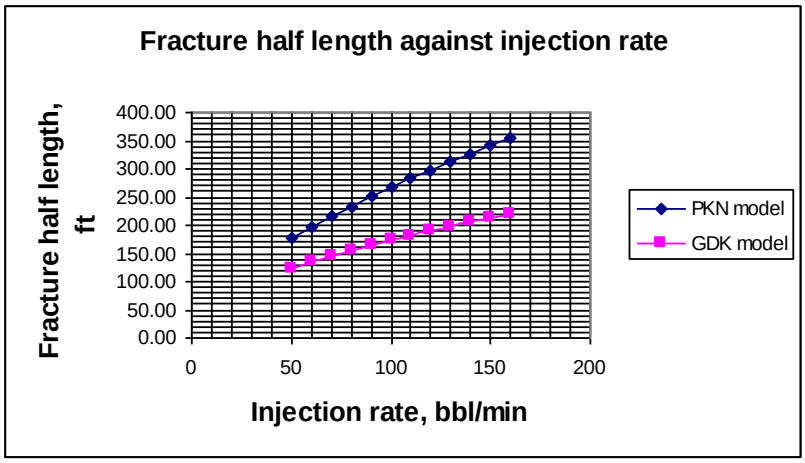

Figure 11- Comparison between PKN and GDK models for fracture half length on parameter injection rate.

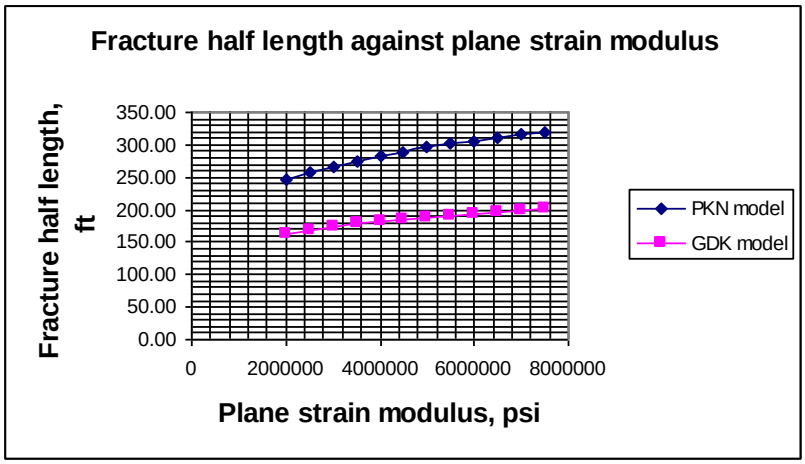

Figure 12- Comparison between PKN and GDK models for fracture half length on parameter plane strain modulus.

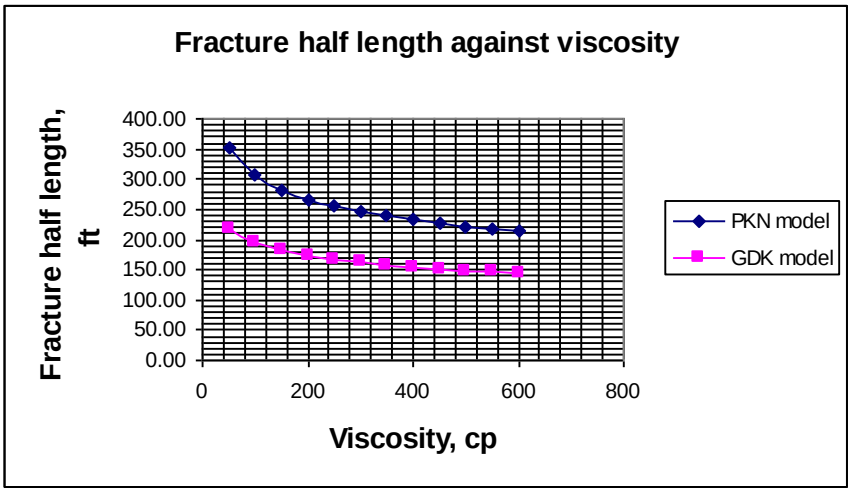

Figure 13- Comparison between PKN and GDK models for fracture half length on parameter viscosity.

In all cases, it can be observed that the PKN model predicts a larger fracture half length compared to GDK model, agreeing to the papers reviewed. The PKN and GDK models show similar trends. Increase in time, injection rate and plane strain modulus increases fracture half length initially linearly then it begins to plateau. An increase in fracture height and viscosity, however, shows decrease in fracture half length then it begins to plateau.

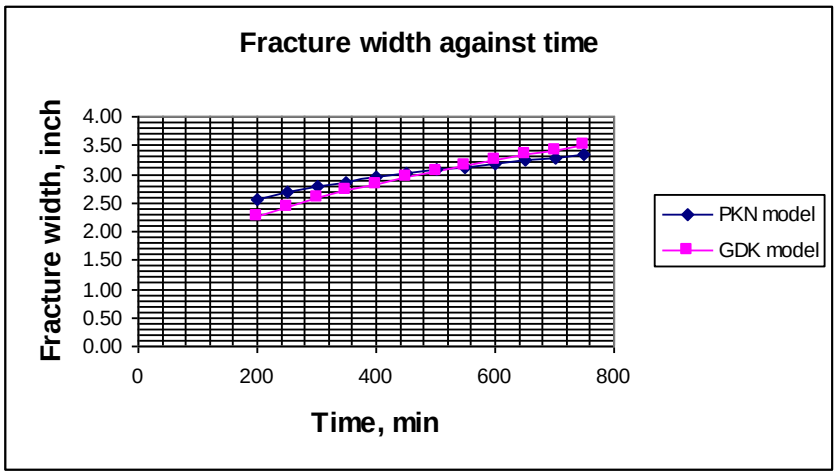

Figure 14- Comparison between PKN and GDK models for fracture width on parameter time.

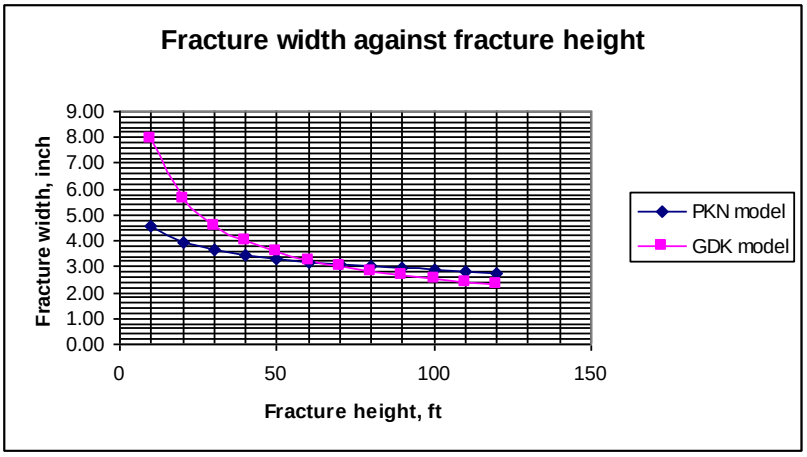

Figure 15- Comparison between PKN and GDK models for fracture width on parameter fracture height.

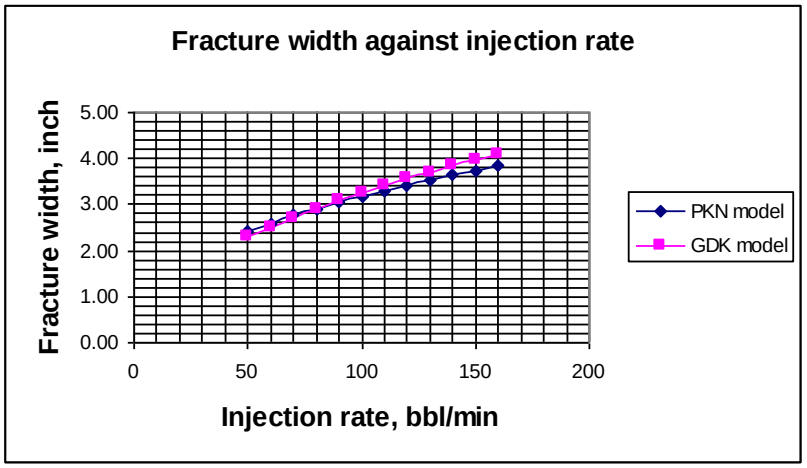

Figure 16- Comparison between PKN and GDK models for fracture width on parameter injection rate.

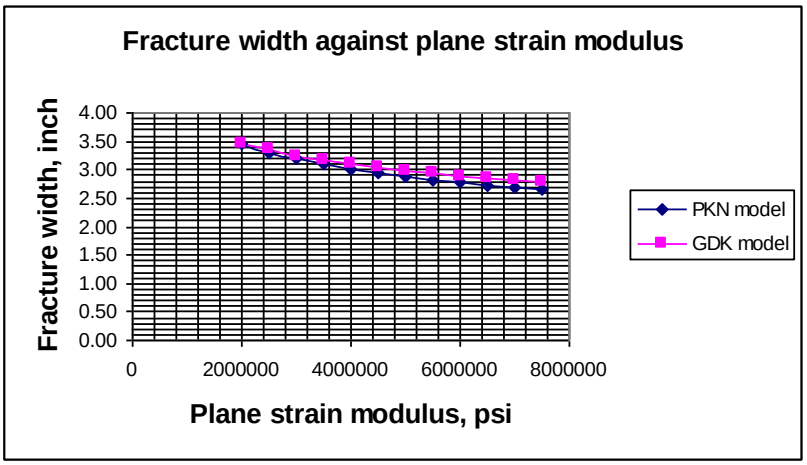

Figure 17- Comparison between PKN and GDK models for fracture width on parameter plane strain modulus.

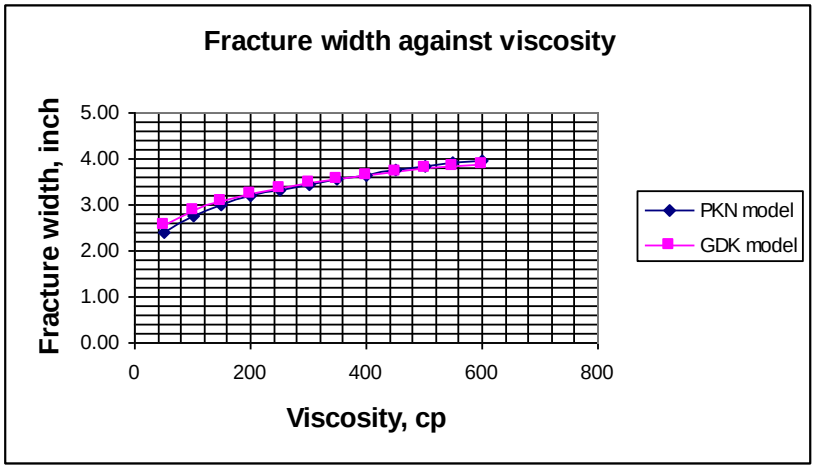

Figure 18- Comparison between PKN and GDK models for fracture width on parameter viscosity.

In all cases, the fracture width generated by PKN and GDK models show relatively close results; however, it can be observed that the GDK model predicts slightly larger fracture width values compared to PKN model, agreeing to the papers reviewed. The PKN and GDK models also show similar trends for fracture width. Increasing time, injection rate and viscosity increases fracture width while increasing fracture height and plane strain modulus decreases fracture width.

To sum up the effects of variation in parameters, it is found that increasing injection rate and time increases fracture half length and fracture width; increasing fracture height reduces both fracture half length and fracture width; increasing plane strain modulus increases fracture half length but decreases fracture width, and increasing viscosity decreases fracture half length but increases fracture width.

Tables of values are included in Appendix C.

4.1.2 PKN Model and UFD

The result for base case is shown in Table 7. Parameters time, fracture height, injection rate, plane strain modulus, viscosity, proppant pack permeability and reservoir permeability have been investigated and Figures 19 to 25 are produced respectively.

Table 7- Optimization study result for hypothetical base case of PKN model.

Parameter	Value	Unit
Case	1- High efficiency	-
Fracture half length	266.86	ft
Fracture width at wellbore	3.19	in
Penetration ratio	0.27	-
Dimensionless fracture conductivity	358159.63	-
Proppant Number	25506.00	-
Dimensionless productivity index	2.00	-

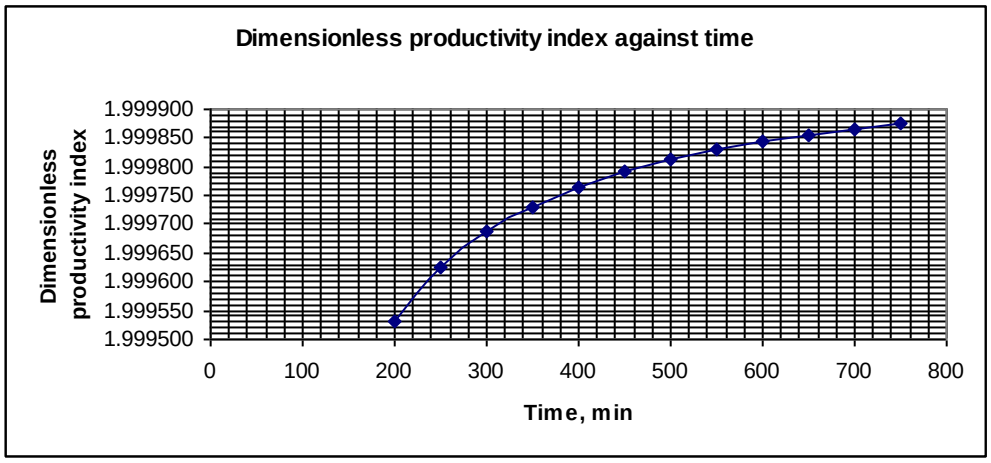

Figure 19- Dimensionless productivity index against time using UFD from PKN model.

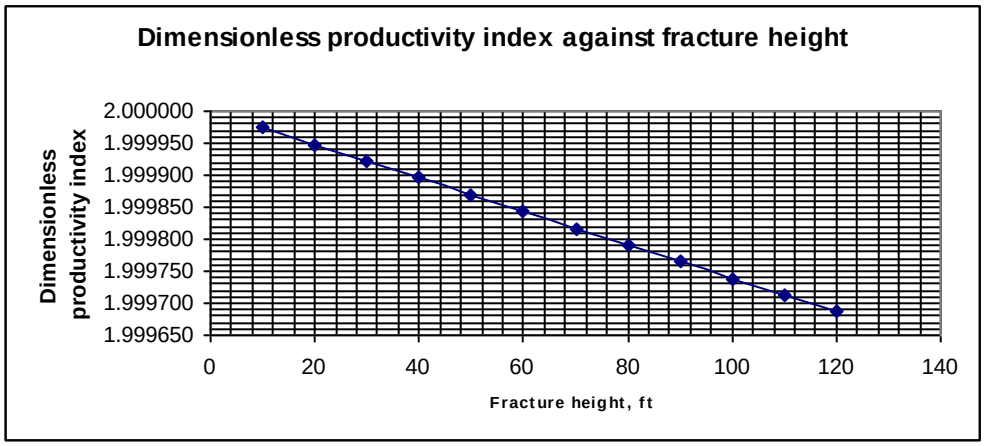

Figure 20- Dimensionless productivity index against fracture height using UFD from PKN model.

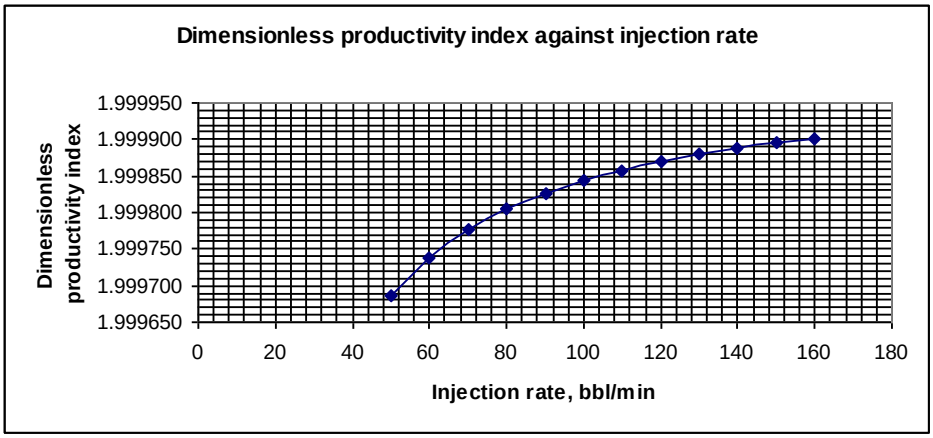

Figure 21- Dimensionless productivity index against injection rate using UFD from PKN model.

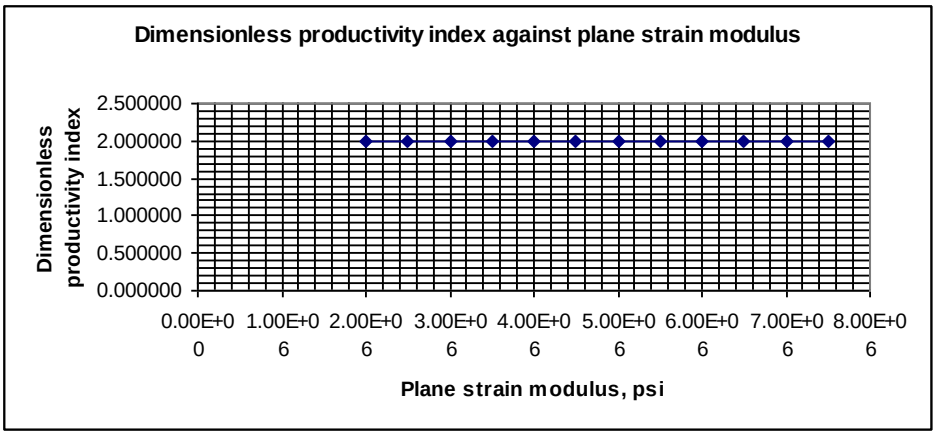

Figure 22- Dimensionless productivity index against plane strain modulus using UFD from PKN model.

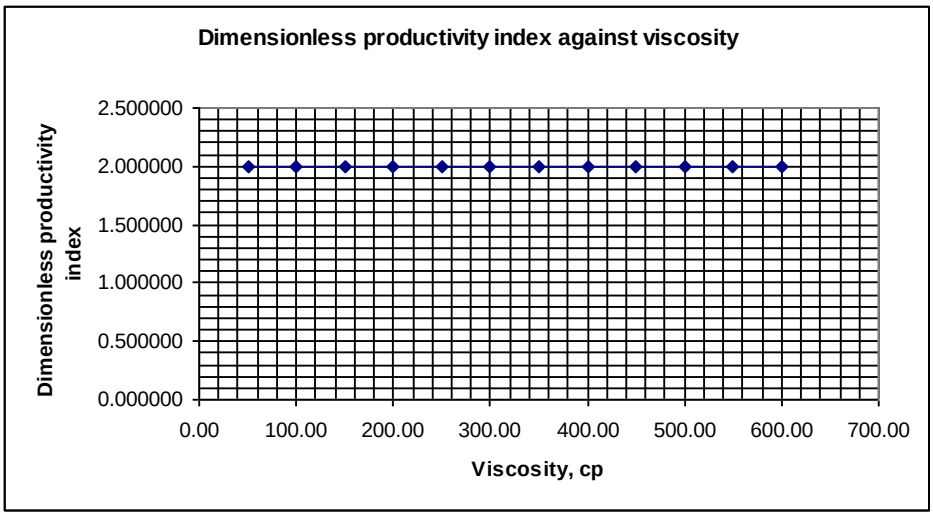

Figure 23- Dimensionless productivity index against viscosity using UFD from PKN model.

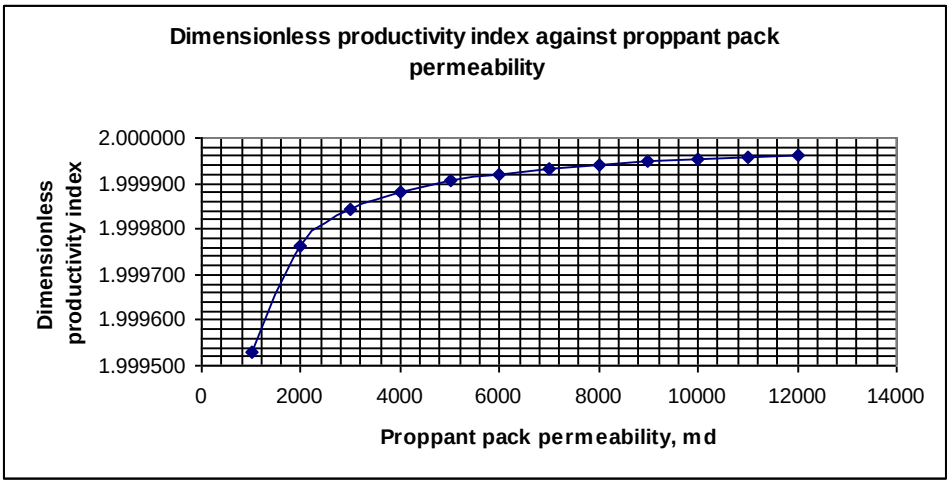

Figure 24- Dimensionless productivity index against proppant pack permeability using UFD from PKN model.

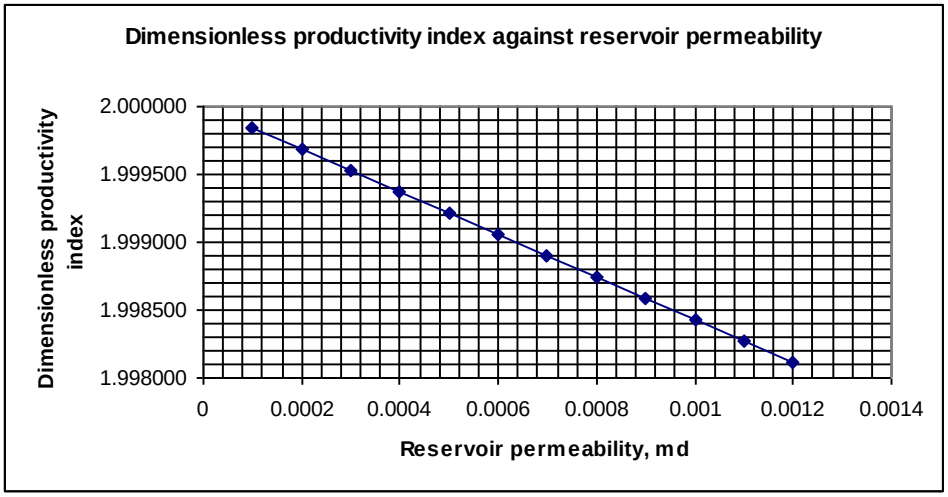

Figure 25- Dimensionless productivity index against reservoir permeability using UFD from PKN model.

It can be observed that increasing time, injection rate and proppant pack permeability increases the dimensionless productivity index until it begins to plateau. An increase in reservoir permeability and fracture height, however, reduces the dimensionless productivity index almost linearly. No considerable change in dimensionless productivity index is observed for plane strain modulus and viscosity variation. The maximum dimensionless productivity index achievable is approximately 2.00. Other considerations such as economic factor may be needed for finalized optimization treatment.

When setting at 50% more than the base case input data for parameter under study using the PKN model and UFD, the plot, as shown in Figure 26, shows that proppant pack permeability, injection rate and time are equally sensitive, about 0.0026% increase of dimensionless productivity index. However, parameters fracture height and reservoir permeability show equal sensitiveness and larger reduction, that is, about 0.0039% less. As expected, parameters viscosity and plane strain modulus are not sensitive to the change of 50%.

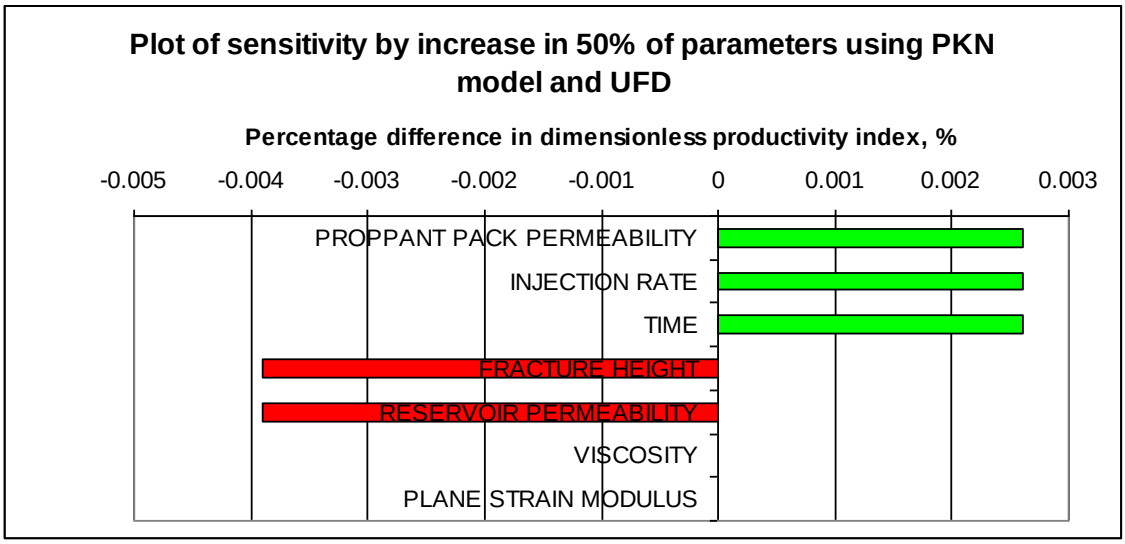

Figure 26- Effect of 50% increase in base case input parameters for PKN model and UFD.

4.1.3 GDK Model and UFD

The maximum dimensionless productivity index is a factor to indicate the ideal requirement to optimize production for optimization study. However, similarly to PKN model results, other considerations such as economic factor may be needed for finalized optimization treatment which is beyond the scope of this study. The result for base case is shown in Table 8. Parameters time, fracture height, injection rate, plane strain modulus, viscosity, proppant pack permeability and reservoir permeability have been investigated and Figures 27 to 33 respectively are produced.

Table 8- Optimization study result for hypothetical base case of GDK model.

Parameter	Value	Unit
Case	1- No leakoff	-
Fracture half length	173.31	ft
Fracture width at wellbore	3.25	in
Penetration ratio	0.17	-
Dimensionless fracture conductivity	561718.25	-
Proppant Number	16872.00	-
Dimensionless productivity index	2.00	-

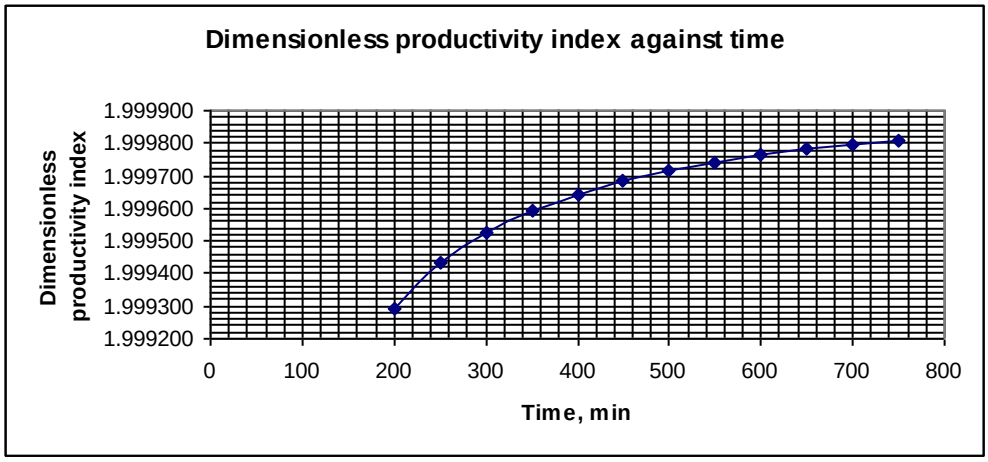

Figure 27- Dimensionless productivity index against time using UFD from GDK model.

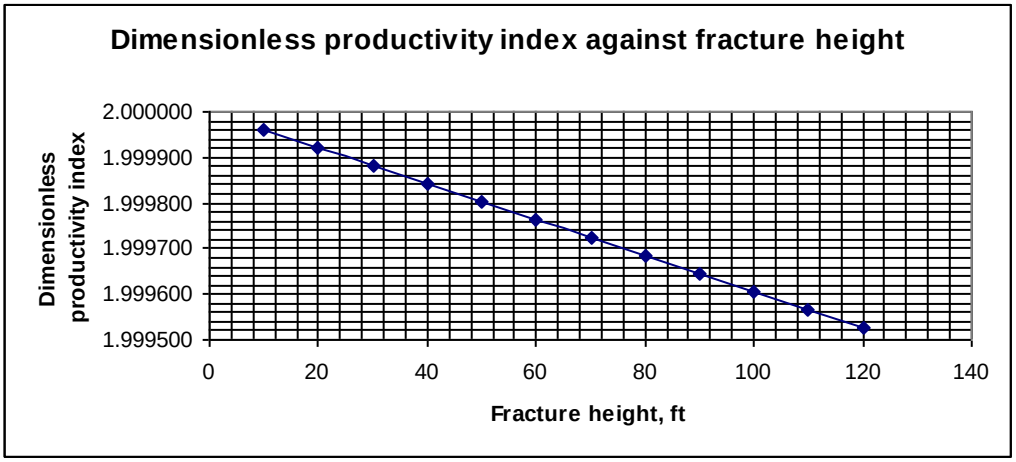

Figure 28- Dimensionless productivity index against fracture height using UFD from GDK model.

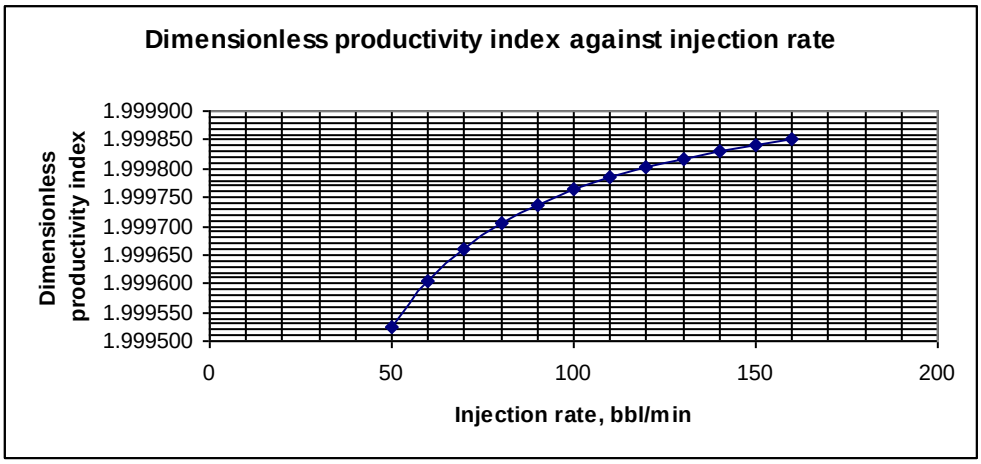

Figure 29- Dimensionless productivity index against injection rate using UFD from GDK model.

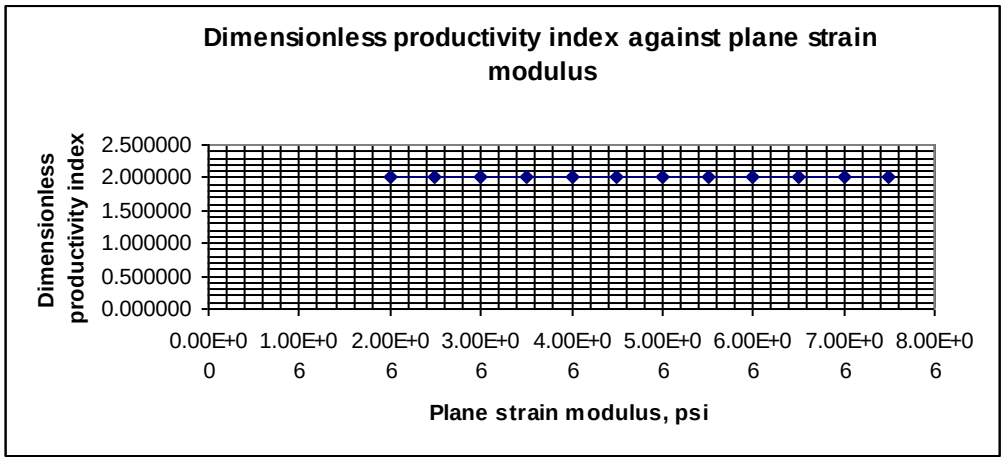

Figure 30- Dimensionless productivity index against plane strain modulus using UFD from GDK model.

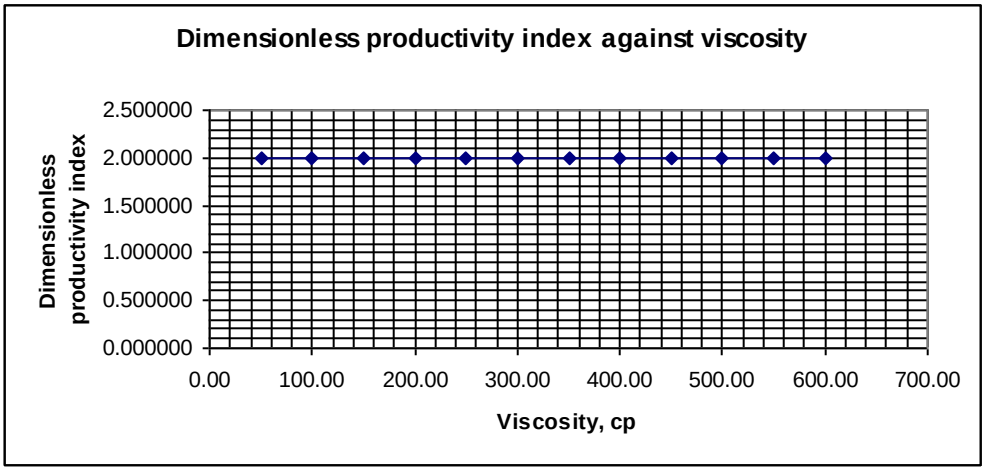

Figure 31- Dimensionless productivity index against viscosity using UFD from GDK model.

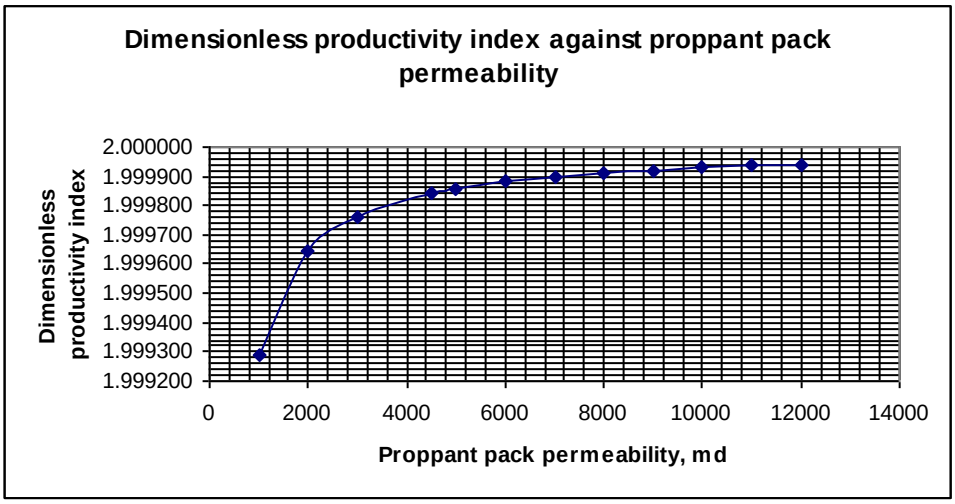

Figure 32- Dimensionless productivity index against proppant pack permeability using UFD from GDK model.

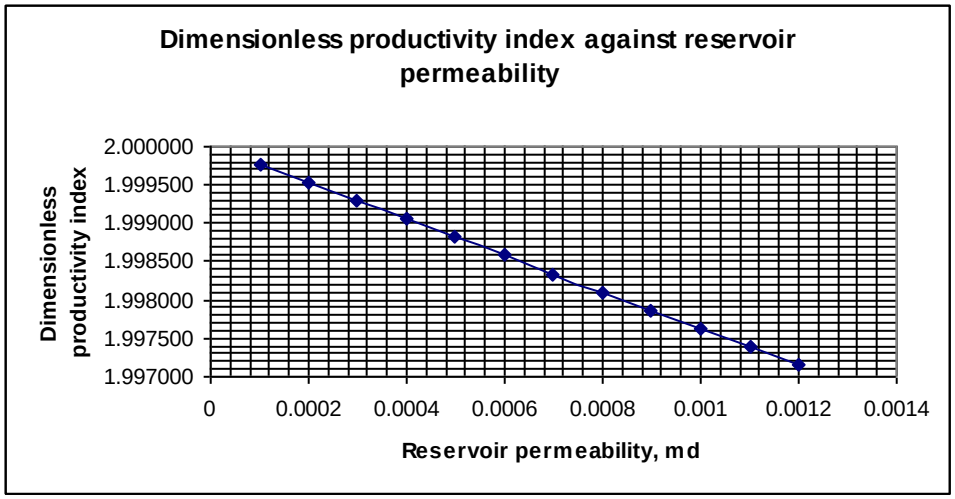

Figure 33- Dimensionless productivity index against reservoir permeability using UFD from GDK model.

It is observed that results for GDK model show similar trends to that using PKN model. Increasing time, injection rate and proppant pack permeability increases the dimensionless productivity index until it begins to plateau; an increase in reservoir permeability and fracture height show reduction in the dimensionless productivity index almost linearly and no considerable change in dimensionless productivity index is seen for plane strain modulus and viscosity variation. The maximum dimensionless productivity index achievable is 2.00.

Similarly, for the GDK model and UFD, a plot is produced to show the sensitivity of parameters that is, when each parameter is set at 50% more than the base case input data, as shown in Figure 34. As mentioned that the trends for the PKN and GDK models sensitivity cases are similar, it can be seen that proppant pack permeability, injection rate and time are equally sensitive, about 0.004% increase of dimensionless productivity index. Parameters fracture height and reservoir permeability show equally sensitive and larger decrease, that is, about 0.0059% less. As expected, parameters viscosity and plane strain modulus are not sensitive to the change of 50%.

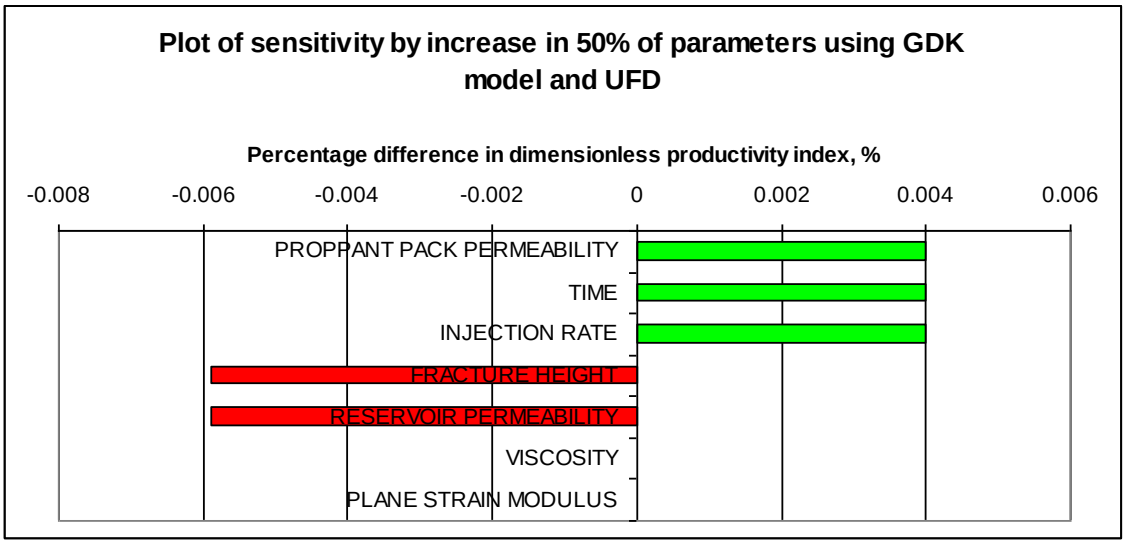

Figure 34- Effect of 50% increase in base case input parameters for GDK model and UFD.

From these studies, we observe that each parameter for the case-specific PKN and GDK models affects the fracture half length and fracture width at the wellbore, which influences the dimensionless productivity index except for plane strain modulus and viscosity parameters. Hence, it is imperative to acquire correct information pertaining to reservoir properties such as the reservoir permeability, fracturing treatment designs like time, injection rate and proppant pack permeability, and identify the fracture height of the formation before simulation work begins to avoid errors in estimating fracture geometry and dimensionless productivity index. Table of values for optimization study using PKN and GDK models are included in Appendix C.

To sum up for the optimization study, the trends of results between the PKN and GDK models show similarity; however, it can be seen that generally, the PKN model predicts a higher dimensionless productivity index compared to the GDK model. This may be because of the PKN model predicting a larger fracture half length and shorter fracture width compared to the GDK model in almost all parameters. Refer Appendix D for illustration of results for comparison of dimensionless productivity index in optimization study's sensitivity studies for both the PKN and GDK models.

4.1.4 Sensitivity Study on Aspect Ratio

An attempt has been made to further investigate hydraulic fracturing in shale oil reservoirs by studying the case of multiple fractures through varying of the aspect ratio. Paper by Bhattacharya, Nikolaou and Economides (2012) writes that the maximum dimensionless productivity index can be approximated by Equation 4.1. Table 9 shows results using both PKN and GDK models that correspond to the statement, that is, the calculated maximum dimensionless productivity index from PKN and GDK models using UFD is close to the theoretical maximum dimensionless productivity index reachable..

$$J_{D,\max} \approx \frac{2}{y_{eD}} \quad \text{.....(4.1)}$$

Table 9- Maximum dimensionless productivity index predicted from PKN and GDK models with comparison to equation provided by the paper.

	From PKN model	**From GDK model**	**From paper**
Aspect ratio	**Dimensionless productivity index**	**Dimensionless productivity index**	**Maximum J_D possible**
0.01	198.46	197.68	200.00
0.02	99.60	99.40	100.00
0.03	66.49	66.39	66.67
0.04	49.90	49.84	50.00
0.05	39.93	39.90	40.00
0.06	33.29	33.26	33.33
0.07	28.54	28.52	28.57
0.08	24.97	24.96	25.00
0.09	22.20	22.19	22.22
0.10	19.98	19.97	20.00
0.11	18.17	18.16	18.18
0.12	16.65	16.65	16.67

4.2 Design Study

In the design study, the optimized fracture half length and fracture width are firstly calculated, and then the required time and injection rate necessary are determined for both Cases 1 and 2 for high efficiency and high leak-off using PKN model, and only Case 1 using GDK model. Table 10 shows the results of base case. For shale oil reservoir where Case 1 is applicable, PKN model estimates time of 7.32E10 min and injection rate of 1.49E-08 bbl/min while GDK estimates time of 1.06E12 min and injection rate of 1.56E-09 bbl/min to achieve an optimized fracture half length and optimized fracture width of 1000.40 ft and 0.015 in respectively.

Table 10- Design study results for hypothetical base case.

Parameter	**Value**	**Unit**
Proppant bulk volume	1860.740	ft3
Proppant number	62024.740	-
Dimensionless fracture conductivity	61975.100	-
Optimized fracture half length	1000.400	ft
Optimized fracture width	0.015	in
PKN Model Case 1 Injection rate	1.49E-08	bbl/min
PKN Model Case 1 Time	7.32E10	min
PKN Model Case 2 Injection rate	1.67E-08	bbl/min
PKN Model Case 2 Time	1.28E22	min
GDK Model Case 1 Injection rate	1.56E-09	bbl/min
GDK Model Case 1 Time	1.06E12	min

Similarly, sensitivity studies are performed for various cases on proppant mass, reservoir permeability, drainage area side length, proppant specific gravity, proppant porosity, proppant pack permeability, plane strain modulus, viscosity, fracture height and aspect ratio. Results are presented in Tables 11 and 12 where the yellow rows denote the base case for analysis. The penetration ratio is found to be close to one; thus, optimized fracture half length is almost half of the drainage area side length for all cases. However, different relationships are observed for optimized fracture width. Increasing proppant mass or proppant porosity increases optimized fracture width while

increasing drainage area side length, proppant specific gravity or fracture height reduces the optimized fracture width. No considerable change is resulted from variation in reservoir permeability, proppant pack permeability and aspect ratio. As expected as plane strain modulus and viscosity parameters are only considered during the calculation of required injection rate and time, no considerable changes are observed for optimized fracture width.

From the tables, it can be concluded that PKN and GDK models show similar trends of results. However, the use of the PKN model generally generates a higher required injection rate to achieve the optimized fracture half length and optimized fracture width compared to the GDK model, while the GDK model estimates a longer time required to achieve the optimized fracture geometry compared to the PKN model for all parameters under study.

It is observed that increasing proppant mass, proppant porosity and plane strain modulus increases the required injection rate with less time required, while the required injection rate decreases and more time is needed when there are increases in drainage area side length, proppant specific gravity, viscosity and fracture height. No considerable changes are observed for required injection rate and time when variations of reservoir permeability, proppant pack permeability and aspect ratio are performed.

Graphical illustrations of the results are enclosed in Appendix E. An attempt to calculate required injection rate and time for Case 2 of the PKN model has been included in Appendix F.

Table 11- Results of parametric studies on proppant mass, reservoir permeability, drainage area side length, proppant specific gravity and proppant porosity.

				PKN model		GDK model	
Parameter	**Value**	**Optimized fracture half length, ft**	**Optimized fracture width, in**	**Injection rate, bbl/min**	**Time, min**	**Injection rate, bbl/min**	**Time, min**
Proppant mass, lbm	100000	1000.4	0.0077	9.34E-10	5.86E+11	9.76E-11	8.47E+12
	200000	1000.4	0.0155	1.49E-08	7.32E+10	1.56E-09	1.06E+12
	300000	1000.4	0.0232	7.57E-08	2.17E+10	7.91E-09	3.14E+11
	400000	1000.4	0.0310	2.39E-07	9.15E+09	2.50E-08	1.32E+11
	500000	1000.4	0.0387	5.84E-07	4.69E+09	6.10E-08	6.78E+10
Reservoir permeability, md	0.00001	1000.4	0.0155	1.49E-08	7.32E+10	1.56E-09	1.06E+12
	0.00005	1000.4	0.0155	1.49E-08	7.32E+10	1.56E-09	1.06E+12
	0.0001	1000.4	0.0155	1.49E-08	7.32E+10	1.56E-09	1.06E+12
	0.00015	1000.4	0.0155	1.49E-08	7.32E+10	1.56E-09	1.06E+12
	0.0002	1000.4	0.0155	1.49E-08	7.32E+10	1.56E-09	1.06E+12
Drainage area side length, ft	1000	500.2	0.0310	4.78E-07	2.29E+09	1.00E-07	1.65E+10
	1500	750.3	0.0207	6.30E-08	1.74E+10	8.78E-09	1.88E+11
	2000	1000.4	0.0155	1.49E-08	7.32E+10	1.56E-09	1.06E+12
	2500	1250.5	0.0124	4.90E-09	2.23E+11	4.10E-10	4.04E+12
	3000	1500.6	0.0103	1.97E-09	5.56E+11	1.37E-10	1.21E+13
Proppant specific gravity	2.50	1000.4	0.0164	1.89E-08	6.15E+10	1.97E-09	8.89E+11
	2.60	1000.4	0.0158	1.61E-08	6.92E+10	1.69E-09	1.00E+12
	2.65	1000.4	0.0155	1.49E-08	7.32E+10	1.56E-09	1.06E+12
	2.70	1000.4	0.0152	1.39E-08	7.74E+10	1.45E-09	1.12E+12
	2.80	1000.4	0.0147	1.20E-08	8.64E+10	1.25E-09	1.25E+12
Proppant porosity	0.20	1000.4	0.0126	6.51E-09	1.37E+11	6.81E-10	1.97E+12
	0.30	1000.4	0.0144	1.11E-08	9.15E+10	1.16E-09	1.32E+12
	0.35	1000.4	0.0155	1.49E-08	7.32E+10	1.56E-09	1.06E+12
	0.40	1000.4	0.0168	2.06E-08	5.76E+10	2.15E-09	8.33E+11
	0.50	1000.4	0.0201	4.27E-08	3.33E+10	4.46E-09	4.82E+11

Table 12- Results of parametric studies on proppant pack permeability, plane strain modulus, viscosity, fracture height and aspect ratio.

				PKN model		GDK model	
Parameter	**Value**	**Optimized fracture half length, ft**	**Optimized fracture width, in**	**Injection rate, bbl/min**	**Time, min**	**Injection rate, bbl/min**	**Time, min**
Proppant pack permeability, md	100000	1000.4	0.0155	1.49E-08	7.32E+10	1.56E-09	1.06E+12
	200000	1000.4	0.0155	1.49E-08	7.32E+10	1.56E-09	1.06E+12
	300000	1000.4	0.0155	1.49E-08	7.32E+10	1.56E-09	1.06E+12
	400000	1000.4	0.0155	1.49E-08	7.32E+10	1.56E-09	1.06E+12
	500000	1000.4	0.0155	1.49E-08	7.32E+10	1.56E-09	1.06E+12
Plane strain modulus, psi	2500000	1000.4	0.0155	1.25E-08	8.79E+10	1.30E-09	1.27E+12
	3000000	1000.4	0.0155	1.49E-08	7.32E+10	1.56E-09	1.06E+12
	3500000	1000.4	0.0155	1.74E-08	6.28E+10	1.82E-09	9.08E+11
	4000000	1000.4	0.0155	1.99E-08	5.49E+10	2.08E-09	7.94E+11
	4500000	1000.4	0.0155	2.24E-08	4.88E+10	2.34E-09	7.06E+11
Viscosity, cp	150	1000.4	0.0155	1.99E-08	5.49E+10	2.08E-09	7.94E+11
	200	1000.4	0.0155	1.49E-08	7.32E+10	1.56E-09	1.06E+12
	250	1000.4	0.0155	1.20E-08	9.15E+10	1.25E-09	1.32E+12
	300	1000.4	0.0155	9.96E-09	1.10E+11	1.04E-09	1.59E+12
	350	1000.4	0.0155	8.54E-09	1.28E+11	8.93E-10	1.85E+12
Fracture height, ft	40	1000.4	0.0232	7.57E-08	1.45E+10	5.27E-09	3.14E+11
	50	1000.4	0.0186	3.10E-08	3.53E+10	2.70E-09	6.13E+11
	60	1000.4	0.0155	1.49E-08	7.32E+10	1.56E-09	1.06E+12
	70	1000.4	0.0133	8.07E-09	1.36E+11	9.84E-10	1.68E+12
	80	1000.4	0.0116	4.73E-09	2.31E+11	6.59E-10	2.51E+12
Aspect ratio	0.10	1000.4	0.0155	1.49E-08	7.32E+10	1.56E-09	1.06E+12
	1.00	1000.4	0.0155	1.49E-08	7.32E+10	1.56E-09	1.06E+12
	0.01	1000.4	0.0155	1.49E-08	7.32E+10	1.56E-09	1.06E+12

To determine the sensitiveness of each parameter in the design study, 50% increase of value of parameter to the base case have been calculated and compared to the base case results. Figures 35 and 36 show the percentage difference for required injection rate and time respectively for PKN model Case 1 while Figures 37 and 38 show the percentage difference for required injection rate and time respectively for GDK model Case 1. As expected, both PKN and GDK models predicted similar results.

For required injection rate, proppant mass is most sensitive, with increase of 406% for both models. Proppant porosity and plane strain modulus show an increase of 250% and 50% respectively for both models. Drainage area side length, proppant specific gravity, fracture height and viscosity all show decrease in percentage difference.

For required time, drainage area side length show the largest difference, that is, 660% and 1040% for PKN and GDK models respectively. Fracture height, proppant specific gravity and viscosity show positive increase for both models while proppant mass, proppant porosity and plane strain modulus show negative differences. With this, it is observed that the relationship between the required injection rate is inverse to time. As expected, increase of 50% for parameters aspect ratio, reservoir permeability and proppant pack permeability does not affect the required injection rate and time.

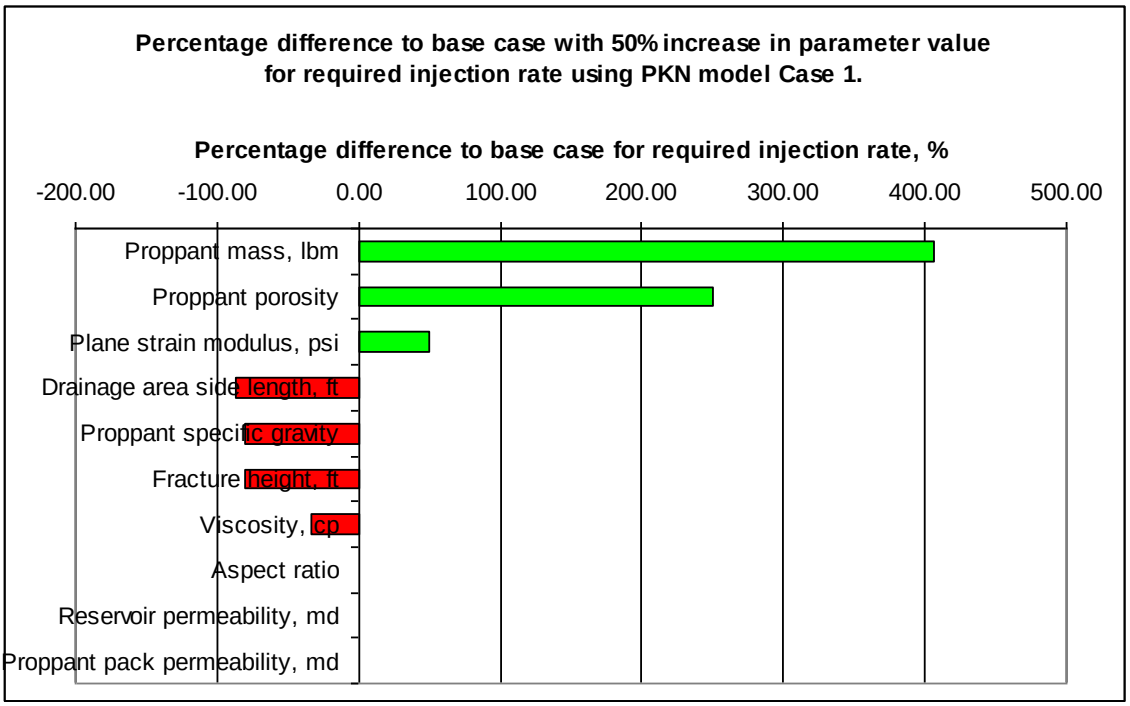

Figure 35- Percentage difference to base case for required injection rate using PKN model Case 1.

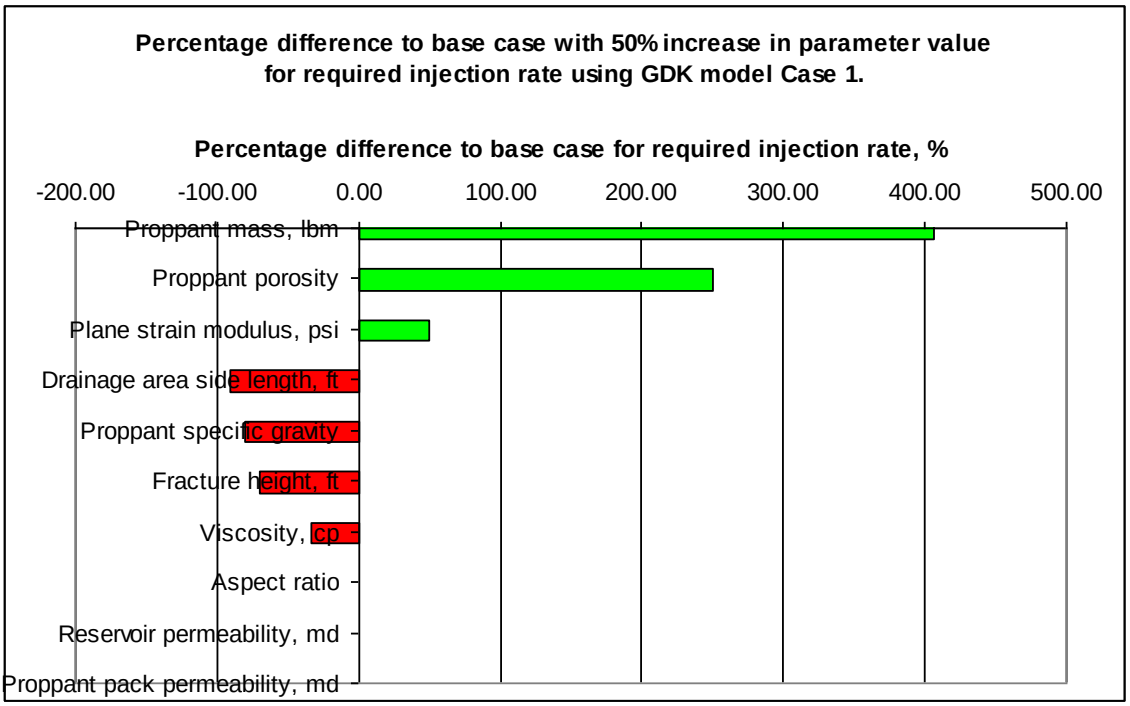

Figure 36 - Percentage difference to base case for required injection rate using GDK model Case 1.

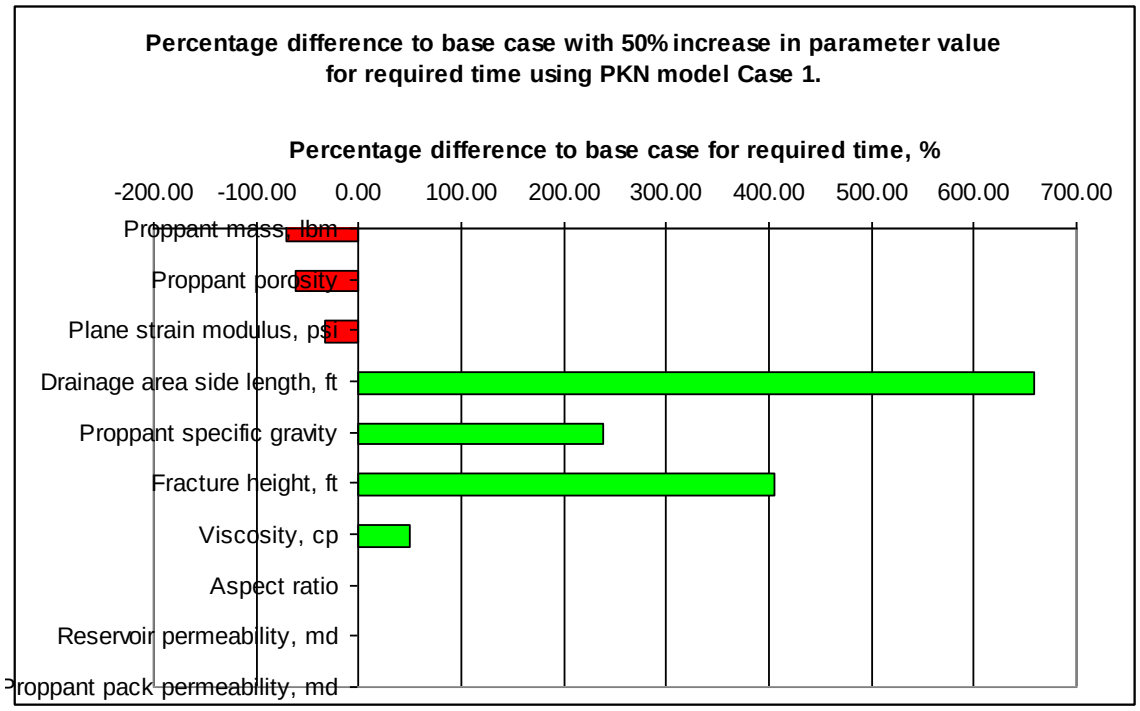

Figure 37- Percentage difference to base case for required time using PKN model Case 1.

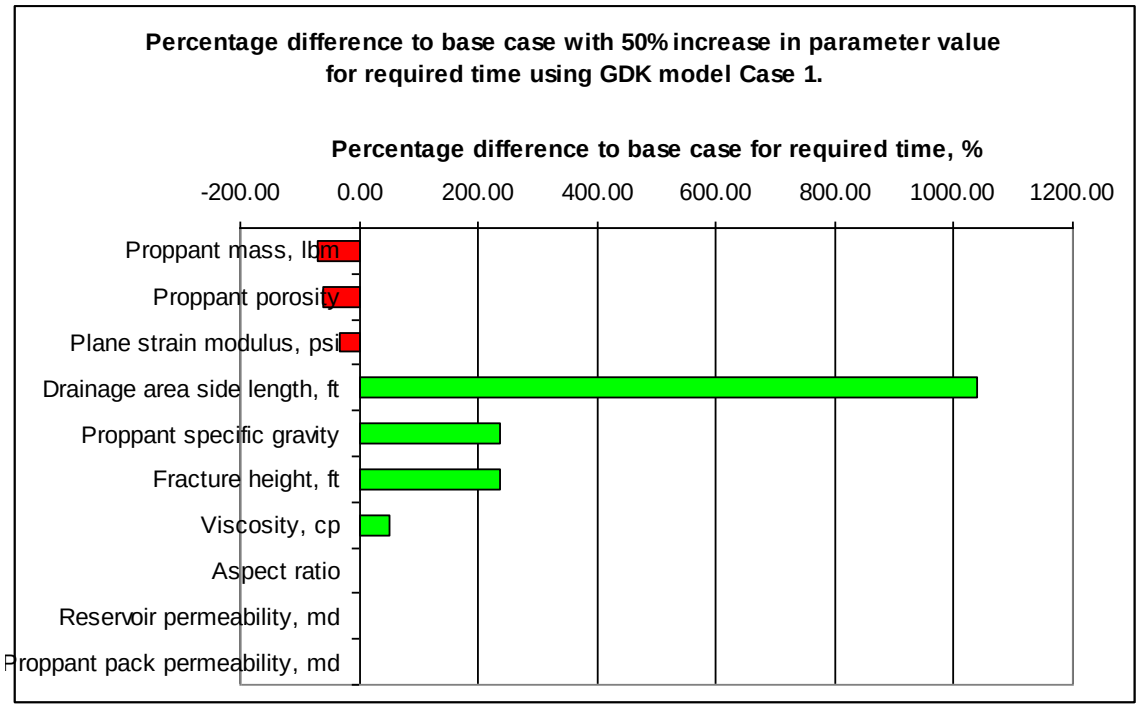

Figure 38- Percentage difference to base case for required time using GDK model Case 1.

CHAPTER 5

CONCLUSIONS AND RECOMMENDATIONS

In this 28-week project, the 2-dimensional PKN and GDK hydraulic fracturing models and the UFD have been selected for the design and optimization study. Sensitivity studies are then performed following the identification of hydraulic fracturing parameters. Several conclusions can be drawn:

- A workflow encompassing the aforementioned models is successfully developed in Microsoft Excel, a key objective of this project.
- In optimization study, using hypothetical base case, the dimensionless productivity indexes calculated are approximately 2.00 for both PKN and GDK models with UFD. The fracture half length and fracture width estimated are 266.86 ft and 3.19 in, and 173.31 ft and 3.25 in for the PKN and GDK models respectively.
- In optimization study, the PKN and GDK models show similar trends in sensitivity analysis, although PKN model generally predicts a longer fracture half length and larger dimensionless productivity index while GDK model estimates larger fracture width, consistent to literature reviewed.
- Dimensionless productivity index increases with increasing time, injection rate and proppant pack permeability, of equal sensitiveness (0.0025% and 0.0040% for PKN and GDK models for 50% increase of each parameter), while it decreases with increasing fracture height and reservoir permeability of equal sensitiveness (-0.004% and -0.006% for PKN and GDK models for 50% increase of each parameter). Parameters plane strain modulus and viscosity are not sensitive.

- In design study, using simultaneous equation method, the injection rate and time required to achieve optimized fracture geometry are determined. Results from hypothetical base case show that it requires 1.49E-08 bbl/min and 7.32E10 min using UFD-PKN, and 1.56E-09 bbl/min and 1.06E12 min using UFD-GDK to achieve optimized fracture half length and width of 1000.4 ft and 0.015 in respectively.
- The PKN model predicts higher injection rate while the GDK model estimates longer time to achieve optimized fracture half length and fracture width. With 50% increase of parameter value to base case, the required injection rate is most sensitive to proppant mass, 406% increase for both PKN and GDK models, while for the required time, it is most sensitive to drainage area side length, increase of 660% and 1040% using PKN and GDK models respectively. Paramters aspect ratio, reservoir permeability and proppant pack permeability are not sensitive.
- Noticeable differences in results using the PKN or GDK model with UFD in both the optimization and design studies.

Hence, it is vital to ensure correct and actual data has been obtained for accurate estimation of stimulation in design and optimization for shale oil reservoir. With these, the objectives of this project have been achieved. The findings of this project provide insights on the effects of parameter variations through quantitative results, heighten the knowledge, and contribute to research development on hydraulic fracturing design and optimization for shale oil reservoirs.

Some recommendations for future studies are:

- Economic analysis;
- Environmental impacts of hydraulic fracturing in shale oil reservoir, particularly on the amount of water consumed; and
- Study on shale oil production.

REFERENCES

1. S. Janwadkar (2004). *Fracture Pressure Analysis of Diagnostic Pump-In Tests of Red Fork Sands in Western Oklahoma.* University of Oklahoma, US.

2. D. Gordon (2012). *Understanding Unconventional Oil,* retrieved from http://www.carnegieendowment.org/files/unconventional_oil.pdf, 24 February 2013.

3. R. Koppelaar (2012). *Shale oil: The latest insights*. Retrieved from http://www.resilience.org/stories/2012-10-26/shale-oil-the-latest-insights# on 27 June 2013.

4. T.T. Palisch, M.A. Chapman and J. Godwin (2012). *Hydraulic Fracture Design Optimization in Unconventional Reservoirs- A Case History*. Presented at SPE Annual Technical Conference and Exhibition, Texas, USA, October 2012, paper SPE 160206

5. J. Baihly, R. Altman and I. Aviles (2012). *Has the Economic Stage Count Been Reached in the Bakken Shale?*. Presented at SPE Hydrocarbon, Economics and Evaluation Symposium, Alberta, Canada, September 2012, paper SPE 159683

6. R.L. Kennedy, R. Gupta, S. Kotov, W.A. Burton, W.N. Knecht and U. Ahmed (2012). *Optimized Shale Resource Development: Proper Placement of Wells and Hydraulic Fracture Stages*. Presented at Abu Dhabi International Petroleum Exhibition & Conference, Abu Dhabi, UAE, November 2012, paper SPE 162534

7. G.E. King (2010). *Thirty Years of Gas Shale Fracturing: What Have We Learned?*. Presented at SPE Annual Technical Conference and Exhibition, Florence, Italy, September 2010, paper SPE 133456

8. J.L. Gidley, S.A. Holditch, D.E. Nierode and R.W. Veatch Jr. (1989) *Recent Advances in Hydraulic Fracturing*. Monograph Series, SPE, Richardson, TX.

9. S.A. Holditch (2006). Presentation materials on Hydraulic Fracturing. NExT.

10. G.E. King (2012). *Hydraulic Fracturing 101: What Every Representative, Environmentalist, Regulator, Reporter, Investor, University Researcher, Neighbour and Engineer Should Know About Estimating Frac Risk and Improving Frac Performance in Unconventional Gas and Oil Wells.* Present at SPE Hydraulic Fracturing Technology Conference, Texas, USA, February 2012, paper SPE 152596

11. D. Ilk, DeGolyer, MacNaughton, N.J. Broussard and T.A. Blasingame (2012). *Production Analysis in the Eagle Ford Shale- Best Practices for Diagnostic*

Interpretations, Analysis, and Modeling. Presented at SPE Annual Technical Conference and Exhibition, Texas, USA, October 2012, paper SPE 160076

12. A. Orangi, N.R. Nagarajan, M.M. Honarpour and J. Rosenzweig (2011). *Unconventional Shale Oil and Gas-Condensate Reservoir Production, Impact of Rock, Fluid, and Hydraulic Fractures*. Presented at SPE Hydraulic Fracturing Technology Conference and Exhibition, Texas, USA, January 2011, paper SPE 140536

13. S.A. Cox, D.M. Cook, K. Dunek, R. Daniels, C. Jump and B. Barree (2008). *Unconventional Resource Play Evaluation: A Look at the Bakken Shale Play of North Dakota*. Presented at SPE Unconventional Reservoirs Conference, Colorado, USA, February 2008, paper SPE 114171

14. C.D. Pope, T. Palisch and P. Saldungaray. (2012). *Improving Completion and Stimulation Effectiveness in Unconventional Reservoirs- Field Results in the Eagle Ford Shale of North America*. Presented at SPE/EAGE European Unconventional Resources Conference and Exhibition, Vienna, Austria, March 2012, paper SPE 152839

15. P. Behr (2013). *Shale Oil: Oil boom masks technological limits that could stifle long-term Bakken potential*. Retrieved from http://www.eenews.net/stories/1059982389 on 27 June 2013.

16. Sam (2012). Waterfloods: The Next Big Profit Phase of the Shale Oil Revolution. Retrieved from http://oilandgas-investments.com/2012/energy-services/waterfloods-the-next-big-profit-phase-of-the-shale-revolution/ on 27 June 2013.

17. Z. Rahim and S.A. Holditch (1993). *Using a Three-Dimensional Concept in a Two-Dimensional Model To Predict Accurate Hydraulic Fracture Dimensions*. Presented at Eastern Regional Conference & Exhibition, PA, USA, November 1993, paper SPE 26926

18. D.E. Nierode (1985). *Comparison of Hydraulic Fracture Design Methods to Observed Field Results*, paper SPE 12059

19. M. Yang, P.P. Valko, and M.J. Economides (2012). *On the Fracture Height Migration under Unified Fracture Design Optimization.* Presented at SPE Canadian Unconventional Resources Conference, Alberta, Canada, November 2012, paper SPE 161641

20. S. Bhattacharya, M. Nikolaou, and M.J. Economides (2012). *Unified Fracture Design for very low permeability reservoirs*. Journal of Natural Gas Science and Engineering, **9**, 184-195

21. *Final Year Project Guidelines for Supervisors and Students* (2012), Version 4.0, Universiti Teknologi PETRONAS

APPENDIX

Appendix A: Snapshots of Spreadsheet

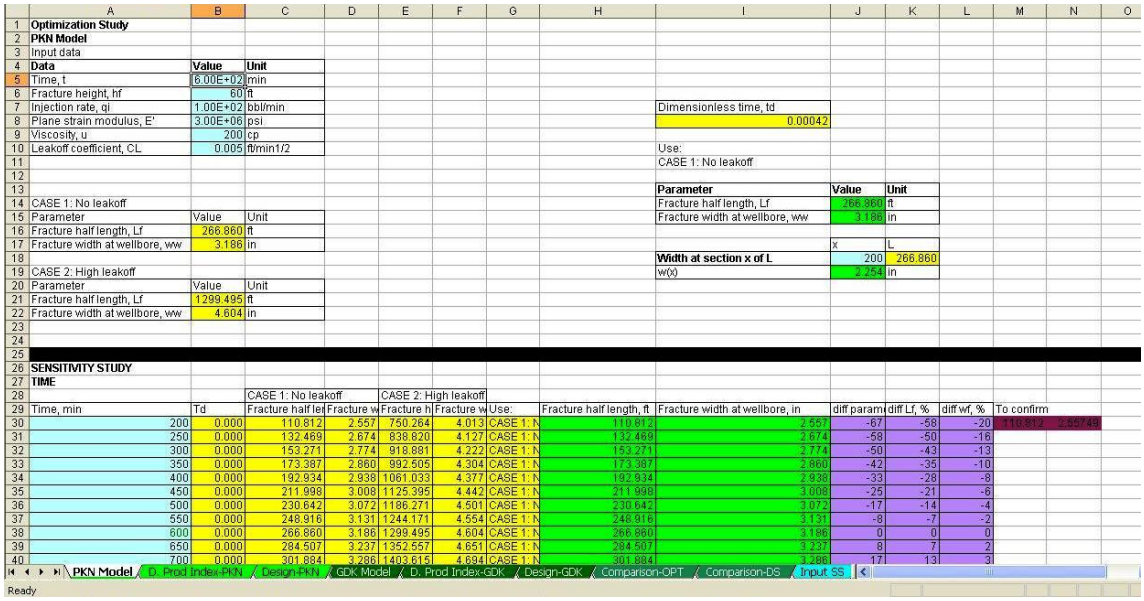

Optimization Study															
PKN Model															
Input data															
Data	Value	Unit													
Time, t	6.00E+02	min													
Fracture height, hf	60	ft													
Injection rate, qi	1.00E+02	bbl/min													
Plane strain modulus, E'	3.00E+06	psi													
Viscosity, u	200	cp													
Leakoff coefficient, CL	0.005	ft/min1/2													
CASE 1: No leakoff															
Parameter	Value	Unit													
Fracture half length, Lf	266.860	ft													
Fracture width at wellbore, ww	3.186	in													
CASE 2: High leakoff															
Parameter	Value	Unit													
Fracture half length, Lf	1299.495	ft													
Fracture width at wellbore, ww	4.604	in													
SENSITIVITY STUDY															
TIME															
			CASE 1: No leakoff		CASE 2: High leakoff										
Time, min	Td		Fracture half length, ft	Fracture width at wellbore, in	Fracture half length, ft	Fracture width at wellbore, in	Use:	Fracture half length, ft	Fracture width at wellbore, in	diff param	diff Lf, %	diff wf, %	To confirm		
200	0.000		110.812	2.557	750.264	4.013	CASE 1: N	110.812	2.557	-67	-58	-20	110.812	2.557	
250	0.000		132.469	2.674	838.820	4.127	CASE 1: N	132.469	2.674	-58	-50	-16			
300	0.000		153.271	2.774	918.881	4.222	CASE 1: N	153.271	2.774	-50	-43	-13			
350	0.000		173.387	2.860	992.505	4.304	CASE 1: N	173.387	2.860	-42	-35	-10			
400	0.000		192.934	2.938	1061.033	4.377	CASE 1: N	192.934	2.938	-33	-28	-8			
450	0.000		211.998	3.008	1125.395	4.442	CASE 1: N	211.998	3.008	-25	-21	-6			
500	0.000		230.642	3.072	1186.271	4.501	CASE 1: N	230.642	3.072	-17	-14	-4			
550	0.000		248.916	3.131	1244.171	4.554	CASE 1: N	248.916	3.131	-8	-7	-2			
600	0.000		266.860	3.186	1299.495	4.604	CASE 1: N	266.860	3.186	0	0	0			
650	0.000		284.507	3.237	1352.557	4.651	CASE 1: N	284.507	3.237	8	7	2			
700	0.000		301.884	3.286	1403.615	4.694	CASE 1: N	301.884	3.286	17	13	3			

Dimensionless time, td
0.00042

Use:
CASE 1: No leakoff

Parameter	Value	Unit
Fracture half length, Lf	266.860	ft
Fracture width at wellbore, ww	3.186	in

	x	L
Width at section x of L	200	266.860
w(x)	2.254	in

Figure 39- Snapshot of the PKN model for optimization study (fracture geometry) in Microsoft Excel.

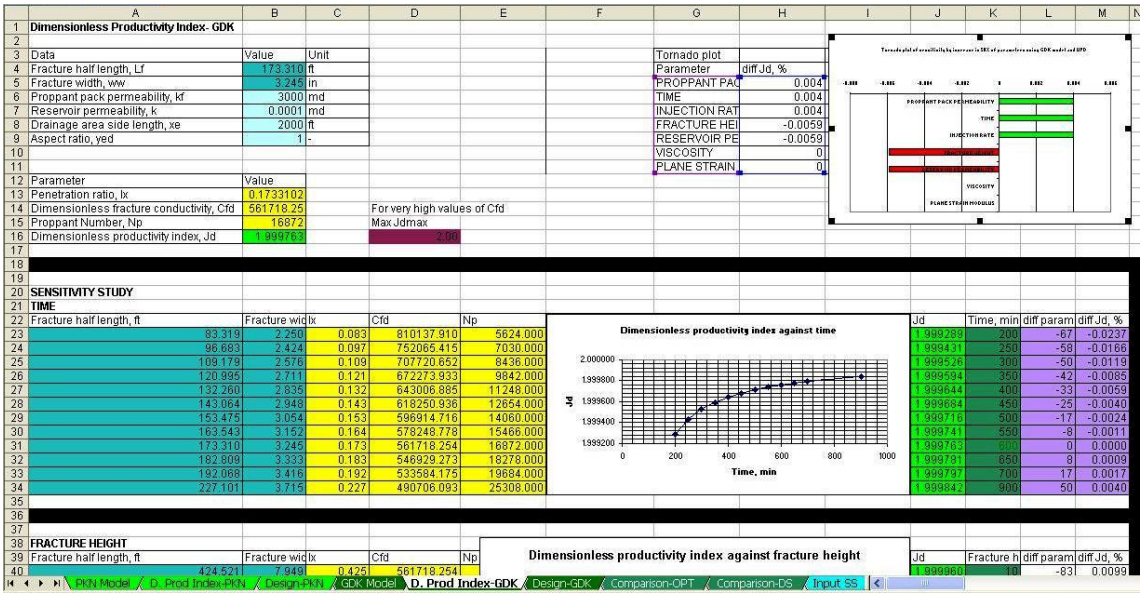

Dimensionless Productivity Index- GDK														
Data	Value	Unit												
Fracture half length, Lf	173.310	ft												
Fracture width, ww	3.245	in												
Proppant pack permeability, kf	3000	md												
Reservoir permeability, k	0.0001	md												
Drainage area side length, xe	2000	ft												
Aspect ratio, yed	1	-												
Parameter	Value													
Penetration ratio, Ix	0.1733102													
Dimensionless fracture conductivity, Cfd	561718.25			For very high values of Cfd										
Proppant Number, Np	16872			Max Jdmax										
Dimensionless productivity index, Jd	1.999763			2.00										
SENSITIVITY STUDY														
TIME														
Fracture half length, ft	Fracture width	Ix	Cfd	Np										
83.319	2.250	0.083	810137.910	5624.000										
96.683	2.424	0.097	752065.415	7030.000										
109.179	2.576	0.109	707720.652	8436.000										
120.995	2.711	0.121	672273.933	9842.000										
132.260	2.835	0.132	643006.885	11248.000										
143.064	2.948	0.143	618250.936	12654.000										
153.475	3.054	0.153	596914.716	14060.000										
163.543	3.152	0.164	578248.778	15466.000										
173.310	3.245	0.173	561718.254	16872.000										
182.809	3.333	0.183	546929.273	18278.000										
192.068	3.416	0.192	533584.175	19684.000										
227.101	3.715	0.227	490706.093	25308.000										
FRACTURE HEIGHT														
Fracture half length, ft	Fracture width	Ix	Cfd	Np										
424.521	7.949	0.425	561718.254											

Tornado plot	
Parameter	diff Jd, %
PROPPANT PAC	0.004
TIME	0.004
INJECTION RAT	0.004
FRACTURE HEI	-0.0059
RESERVOIR PE	-0.0059
VISCOSITY	0
PLANE STRAIN	0

Jd	Time, min	diff param	diff Jd, %
1.999289	200	-67	-0.0237
1.999431	250	-58	-0.0166
1.999526	300	-50	-0.0119
1.999594	350	-42	-0.0085
1.999644	400	-33	-0.0059
1.999684	450	-25	-0.0040
1.999716	500	-17	-0.0024
1.999741	550	-8	-0.0011
1.999763	600	0	0.0000
1.999781	650	8	0.0009
1.999797	700	17	0.0017
1.999842	900	50	0.0040

Jd	Fracture h	diff param	diff Jd, %
1.999960	10	-83	0.0099

Figure 40- Snapshot of the GDK model for optimization study (dimensionless productivity index) in Microsoft Excel.

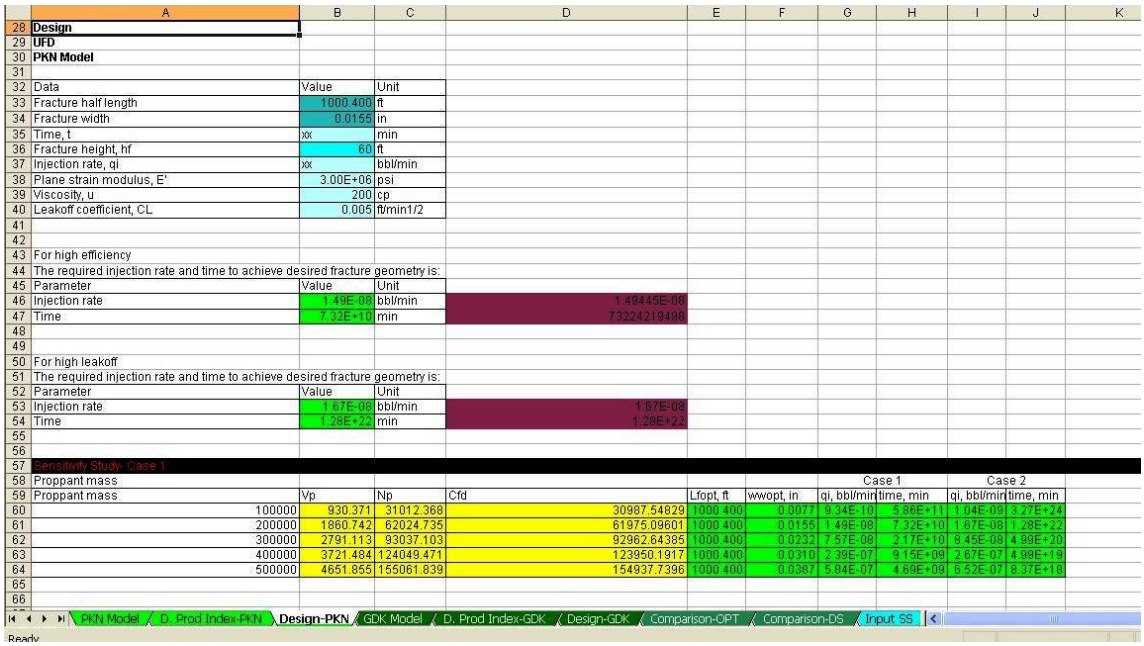

	A	B	C	D	E	F	G	H	I	J	K
28	**Design**										
29	**UFD**										
30	**PKN Model**										
31											
32	Data	Value	Unit								
33	Fracture half length	1000.400	ft								
34	Fracture width	0.0155	in								
35	Time, t	xx	min								
36	Fracture height, hf	60	ft								
37	Injection rate, qi	xx	bbl/min								
38	Plane strain modulus, E'	3.00E+06	psi								
39	Viscosity, u	200	cp								
40	Leakoff coefficient, CL	0.005	ft/min1/2								
41											
42											
43	For high efficiency										
44	The required injection rate and time to achieve desired fracture geometry is:										
45	Parameter	Value	Unit								
46	Injection rate	1.49E-08	bbl/min	1.49445E-08							
47	Time	7.32E+10	min	73224219498							
48											
49											
50	For high leakoff										
51	The required injection rate and time to achieve desired fracture geometry is:										
52	Parameter	Value	Unit								
53	Injection rate	1.67E-08	bbl/min	1.67E-08							
54	Time	1.28E+22	min	1.28E+22							
55											
56											
57	Sensitivity Study- Case 1										
58	Proppant mass							Case 1		Case 2	
59	Proppant mass	Vp	Np	Cfd	Lfopt, ft	wwopt, in	qi, bbl/min	time, min	qi, bbl/min	time, min	
60	100000	930.371	31012.368	30987.54829	1000.400	0.0077	9.34E-10	5.86E+11	1.04E-09	3.27E+24	
61	200000	1860.742	62024.735	61975.09601	1000.400	0.0155	1.49E-08	7.32E+10	1.67E-08	1.28E+22	
62	300000	2791.113	93037.103	92962.64385	1000.400	0.0232	7.57E-08	2.17E+10	8.45E-08	4.99E+20	
63	400000	3721.484	124049.471	123950.1917	1000.400	0.0310	2.39E-07	9.15E+09	2.67E-07	4.99E+19	
64	500000	4651.855	155061.839	154937.7396	1000.400	0.0387	5.84E-07	4.69E+09	6.52E-07	8.37E+18	
65											
66											

PKN Model | D. Prod Index-PKN | Design-PKN | GDK Model | D. Prod Index-GDK | Design-GDK | Comparison-OPT | Comparison-DS | Input SS

Ready

Figure 41- Snapshot of the UFD and PKN model for design study in Microsoft Excel.

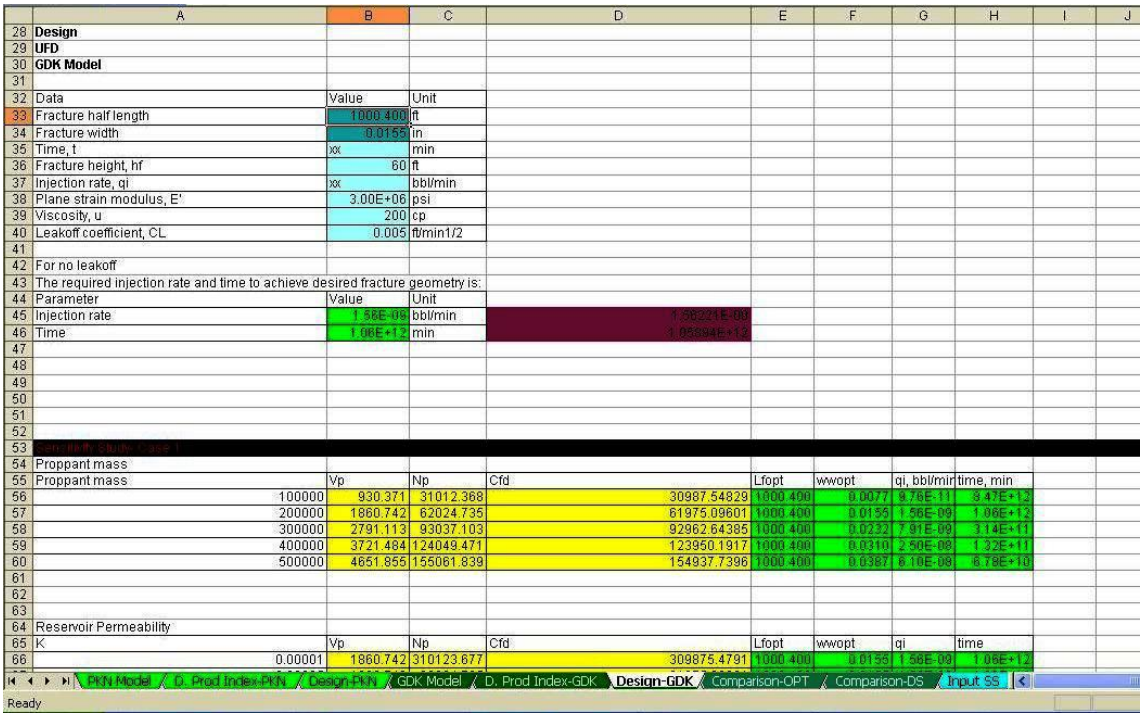

	A	B	C	D	E	F	G	H	I	J
28	**Design**									
29	**UFD**									
30	**GDK Model**									
31										
32	Data	Value	Unit							
33	Fracture half length	1000.400	ft							
34	Fracture width	0.0155	in							
35	Time, t	xx	min							
36	Fracture height, hf	60	ft							
37	Injection rate, qi	xx	bbl/min							
38	Plane strain modulus, E'	3.00E+06	psi							
39	Viscosity, u	200	cp							
40	Leakoff coefficient, CL	0.005	ft/min1/2							
41										
42	For no leakoff									
43	The required injection rate and time to achieve desired fracture geometry is:									
44	Parameter	Value	Unit							
45	Injection rate	1.58E-09	bbl/min	1.58221E-09						
46	Time	1.06E+12	min	1.05894E+12						
47										
48										
49										
50										
51										
52										
53	Sensitivity Study- Case 1									
54	Proppant mass									
55	Proppant mass	Vp	Np	Cfd	Lfopt	wwopt	qi, bbl/min	time, min		
56	100000	930.371	31012.368	30987.54829	1000.400	0.0077	9.76E-11	9.47E+12		
57	200000	1860.742	62024.735	61975.09601	1000.400	0.0155	1.56E-09	1.06E+12		
58	300000	2791.113	93037.103	92962.64385	1000.400	0.0232	7.91E-09	3.14E+11		
59	400000	3721.484	124049.471	123950.1917	1000.400	0.0310	2.50E-08	1.32E+11		
60	500000	4651.855	155061.839	154937.7396	1000.400	0.0387	6.10E-08	6.78E+10		
61										
62										
63										
64	Reservoir Permeability									
65	K	Vp	Np	Cfd	Lfopt	wwopt	qi	time		
66	0.00001	1860.742	310123.677	309875.4791	1000.400	0.0155	1.58E-09	1.06E+12		

PKN Model | D. Prod Index-PKN | Design-PKN | GDK Model | D. Prod Index-GDK | Design-GDK | Comparison-OPT | Comparison-DS | Input SS

Ready

Figure 42- Snapshot of the UFD and GDK model for design study in Microsoft Excel.

Appendix B: Input Data for Sensitivity Study

Table 13- 12 different input values for parameter under study for optimization study sensitivity analysis.

Parameter						
Time, min	**Fracture height, ft**	**Injection rate, bbl/min**	**Plane strain modulus, psi**	**Viscosity, cp**	**Proppant pack permeability, md**	**Reservoir permeability, md**
200	10	50	2000000	50	1000	0.0001
250	20	60	2500000	100	2000	0.0002
300	30	70	3000000	150	3000	0.0003
350	40	80	3500000	200	4000	0.0004
400	50	90	4000000	250	5000	0.0005
450	60	100	4500000	300	6000	0.0006
500	70	110	5000000	350	7000	0.0007
550	80	120	5500000	400	8000	0.0008
600	90	130	6000000	450	9000	0.0009
650	100	140	6500000	500	10000	0.001
700	110	150	7000000	550	11000	0.0011
750	120	160	7500000	600	12000	0.0012

Note: Yellow boxes indicate base case input data.

Table 14- Various input values for parameter under study for design study sensitivity analysis.

Parameter	Value
Proppant mass, lbm	100000
	200000
	300000
	400000
	500000
Reservoir permeability, md	0.00001
	0.00005
	0.0001
	0.00015
	0.0002
Drainage area side length, ft	1000
	1500
	2000
	2500
	3000
Proppant specific gravity	2.5
	2.6
	2.65
	2.7
	2.8
Proppant porosity	0.2
	0.3
	0.35
	0.4
	0.5

Parameter	Value
Proppant pack permeability, md	100000
	200000
	300000
	400000
	500000
Fracture height, ft	40
	50
	60
	70
	80
Plane strain modulus, psi	2500000
	3000000
	3500000
	4000000
	4500000
Viscosity, cp	150
	200
	250
	300
	350
Aspect ratio	0.1
	1
	0.01

Note: Yellow boxes indicate base case input data.

Appendix C: Optimization Study Tabulated Results

Table 15- Table of result for optimization study sensitivity analysis on parameter time.

	PKN			GDK		
Time, min	Fracture half length, ft	Fracture width at wellbore, in	Jd	Fracture half length, ft	Fracture width at wellbore, in	Jd
200	110.81	2.56	1.99953	83.32	2.25	1.99929
250	132.47	2.67	1.99962	96.68	2.42	1.99943
300	153.27	2.77	1.99969	109.18	2.58	1.99953
350	173.39	2.86	1.99973	121.00	2.71	1.99959
400	192.93	2.94	1.99976	132.26	2.83	1.99964
450	212.00	3.01	1.99979	143.06	2.95	1.99968
500	230.64	3.07	1.99981	153.47	3.05	1.99972
550	248.92	3.13	1.99983	163.54	3.15	1.99974
600	266.86	3.19	1.99984	173.31	3.25	1.99976
650	284.51	3.24	1.99986	182.81	3.33	1.99978
700	301.88	3.29	1.99987	192.07	3.42	1.99980
750	319.01	3.33	1.99987	227.10	3.71	1.99984

Table 16- Table of result for optimization study sensitivity analysis on parameter fracture height.

	PKN			GDK		
Fracture height, ft	Fracture half length, ft	Fracture width at wellbore, in	Jd	Fracture half length, ft	Fracture width at wellbore, in	Jd
10	1118.93	4.56	1.999974	424.52	7.95	1.999960
20	642.66	3.97	1.999948	300.18	5.62	1.999921
30	464.63	3.66	1.999922	245.10	4.59	1.999881
40	369.11	3.46	1.999895	212.26	3.97	1.999842
50	308.76	3.30	1.999869	189.85	3.55	1.999802
60	266.86	3.19	1.999843	173.31	3.25	1.999763
70	235.90	3.09	1.999817	160.45	3.00	1.999723
80	212.00	3.01	1.999791	150.09	2.81	1.999684
90	192.93	2.94	1.999765	141.51	2.65	1.999644
100	177.34	2.88	1.999739	134.25	2.51	1.999605
110	164.32	2.82	1.999713	128.00	2.40	1.999565
120	153.27	2.77	1.999686	122.55	2.29	1.999526

Table 17- Table of result for optimization study sensitivity analysis on parameter injection rate.

	PKN			GDK		
Injection rate, bbl/min	**Fracture half length, ft**	**Fracture width at wellbore, in**	**Jd**	**Fracture half length, ft**	**Fracture width at wellbore, in**	**Jd**
50	176.06	2.41	1.999686	122.55	2.29	1.999526
60	196.41	2.60	1.999739	134.25	2.51	1.999605
70	215.45	2.76	1.999776	145.00	2.72	1.999661
80	233.42	2.91	1.999804	155.01	2.90	1.999704
90	250.51	3.05	1.999826	164.42	3.08	1.999737
100	266.86	3.19	1.999843	173.31	3.25	1.999763
110	282.57	3.31	1.999857	181.77	3.40	1.999785
120	297.71	3.43	1.999869	189.85	3.55	1.999802
130	312.36	3.54	1.999879	197.60	3.70	1.999818
140	326.56	3.64	1.999888	205.06	3.84	1.999831
150	340.36	3.75	1.999895	212.26	3.97	1.999842
160	353.80	3.84	1.999902	219.22	4.10	1.999852

Table 18- Table of result for optimization study sensitivity analysis on parameter plane strain modulus.

	PKN			GDK		
Plane strain modulus, psi	**Fracture half length, ft**	**Fracture width at wellbore, in**	**Jd**	**Fracture half length, ft**	**Fracture width at wellbore, in**	**Jd**
2000000	246.07	3.46	1.999843	161.99	3.47	1.999763
2500000	257.30	3.30	1.999843	168.12	3.35	1.999763
3000000	266.86	3.19	1.999843	173.31	3.25	1.999763
3500000	275.22	3.09	1.999843	177.82	3.16	1.999763
4000000	282.66	3.01	1.999843	181.82	3.09	1.999763
4500000	289.40	2.94	1.999843	185.43	3.03	1.999763
5000000	295.56	2.88	1.999843	188.71	2.98	1.999763
5500000	301.25	2.82	1.999843	191.73	2.93	1.999763
6000000	306.54	2.77	1.999843	194.53	2.89	1.999763
6500000	311.49	2.73	1.999843	197.15	2.85	1.999763
7000000	316.14	2.69	1.999843	199.60	2.82	1.999763
7500000	320.53	2.65	1.999843	201.91	2.79	1.999763

Table 19- Table of result for optimization study sensitivity analysis on parameter viscosity.

	PKN			GDK		
Viscosity, cp	**Fracture half length, ft**	**Fracture width at wellbore, in**	**Jd**	**Fracture half length, ft**	**Fracture width at wellbore, in**	**Jd**
50	352.12	2.41	1.999843	218.36	2.58	1.999763
100	306.54	2.77	1.999843	194.53	2.89	1.999763
150	282.66	3.01	1.999843	181.82	3.09	1.999763
200	266.86	3.19	1.999843	173.31	3.25	1.999763
250	255.21	3.33	1.999843	166.98	3.37	1.999763
300	246.07	3.46	1.999843	161.99	3.47	1.999763
350	238.60	3.56	1.999843	157.88	3.56	1.999763
400	232.31	3.66	1.999843	154.40	3.64	1.999763
450	226.91	3.75	1.999843	151.40	3.71	1.999763
500	222.17	3.83	1.999843	148.76	3.78	1.999763
550	217.98	3.90	1.999843	146.42	3.84	1.999763
600	214.22	3.97	1.999843	144.31	3.90	1.999763

Table 20- Table of result for optimization study sensitivity analysis on parameter proppant pack permeability.

	PKN	GDK
Proppant pack permeability, md	**Jd**	**Jd**
1000	1.999530	1.999289
2000	1.999765	1.999644
3000	1.999843	1.999763
4000	1.999882	1.999842
5000	1.999906	1.999858
6000	1.999922	1.999881
7000	1.999933	1.999898
8000	1.999941	1.999911
9000	1.999948	1.999921
10000	1.999953	1.999929
11000	1.999957	1.999935
12000	1.999961	1.999941

Table 21- Table of result for optimization study sensitivity analysis on parameter reservoir permeability.

	PKN	GDK
Reservoir permeability, md	**Jd**	**Jd**
0.0001	1.999843	1.999763
0.0002	1.999686	1.999644
0.0003	1.999530	1.999289
0.0004	1.999373	1.999052
0.0005	1.999216	1.998815
0.0006	1.999060	1.998579
0.0007	1.998903	1.998342
0.0008	1.998746	1.998106
0.0009	1.998590	1.997869
0.001	1.998433	1.997633
0.0011	1.998277	1.997396
0.0012	1.998120	1.997160

Appendix D: Optimization Study J_D Comparison

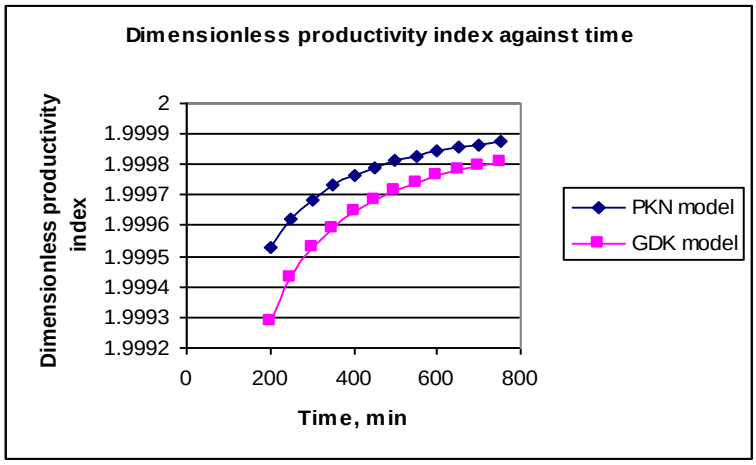

Figure 43- Comparison of dimensionless productivity index between PKN and GDK models for parameter time.

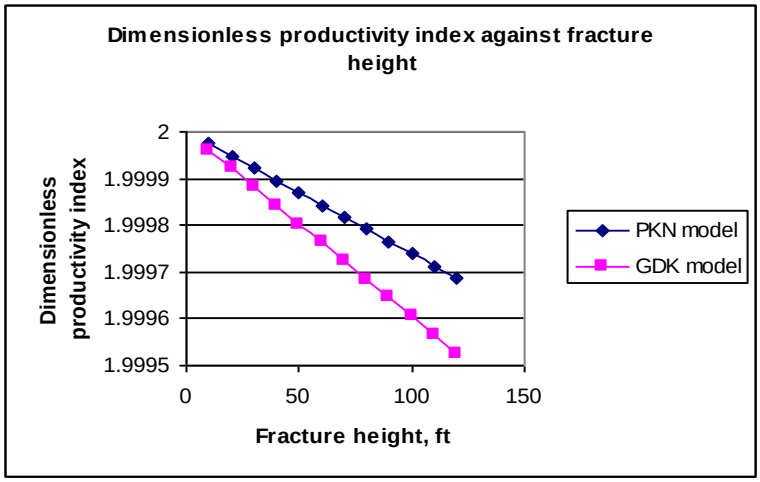

Figure 44- Comparison of dimensionless productivity index between PKN and GDK models for parameter fracture height.

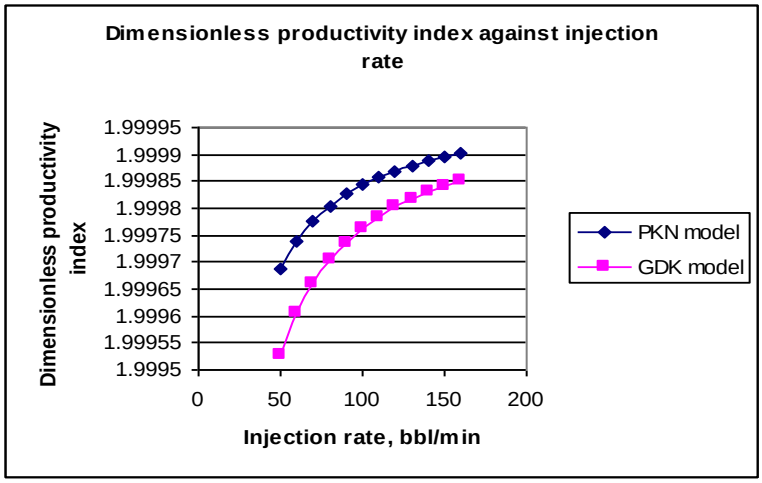

Figure 45- Comparison of dimensionless productivity index between PKN and GDK models for parameter injection rate.

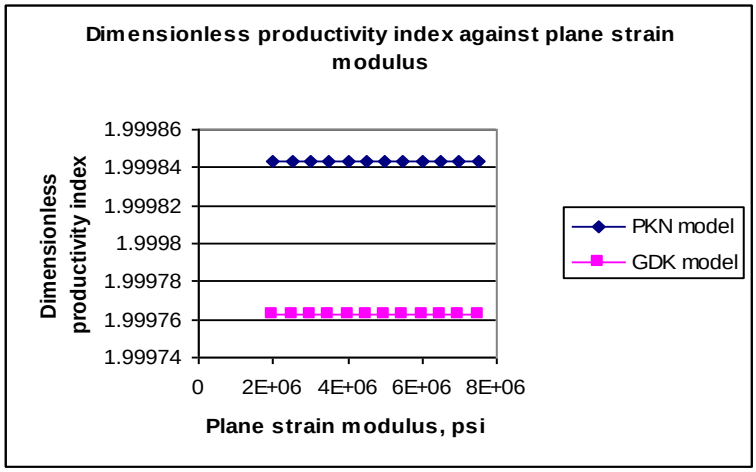

Figure 46- Comparison of dimensionless productivity index between PKN and GDK models for parameter plane strain modulus.

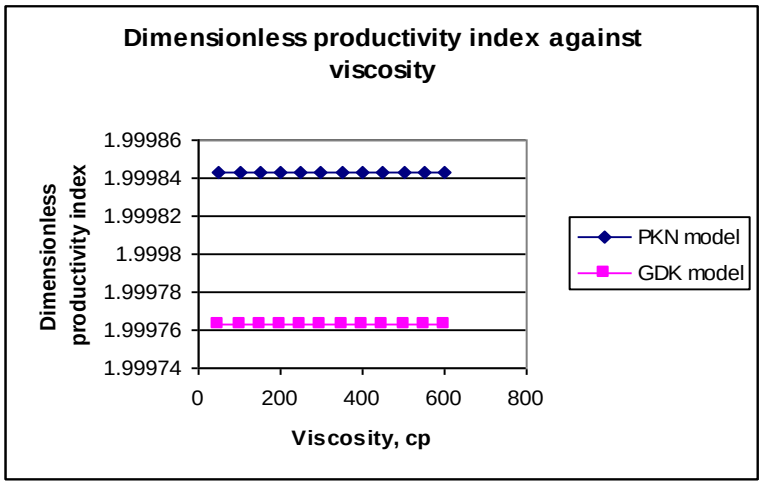

Figure 47- Comparison of dimensionless productivity index between PKN and GDK models for parameter viscosity.

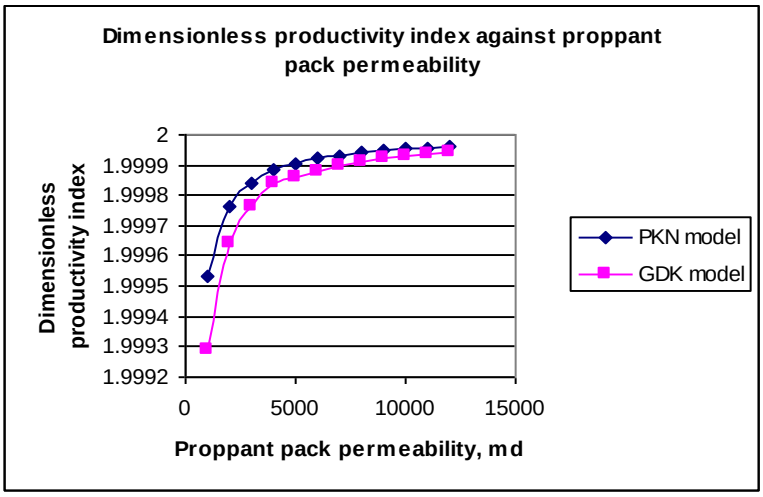

Figure 48- Comparison of dimensionless productivity index between PKN and GDK models for parameter proppant pack permeability.

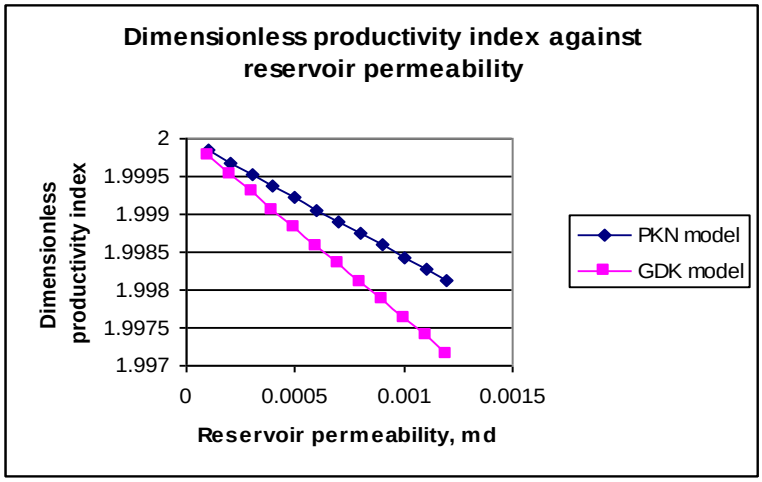

Figure 49- Comparison of dimensionless productivity index between PKN and GDK models for parameter reservoir permeability.

Appendix E: Design Study Case 1 Results

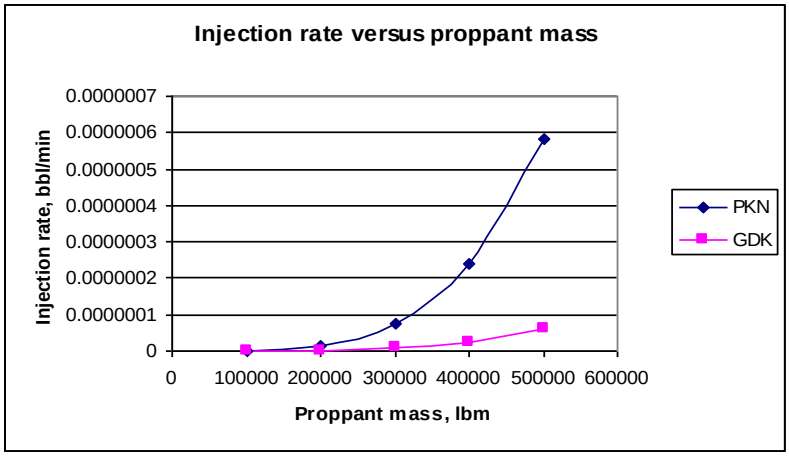

Figure 50- Design study using Case 1 for PKN and GDK models on required injection rate against proppant mass.

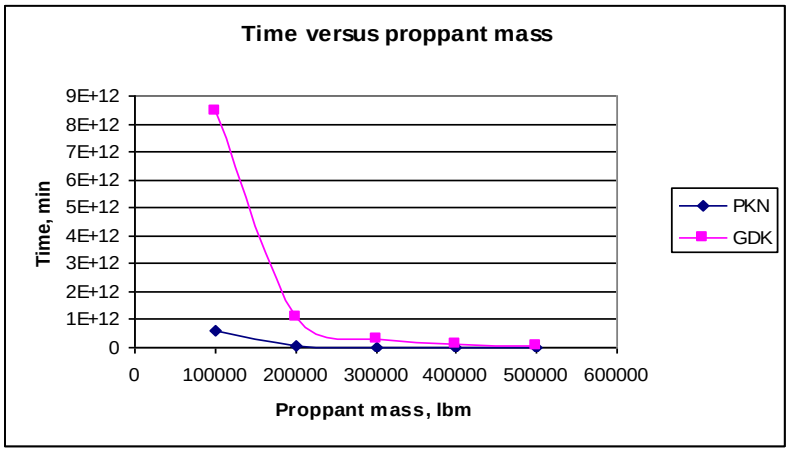

Figure 51- Design study using Case 1 for PKN and GDK models on required time against proppant mass.

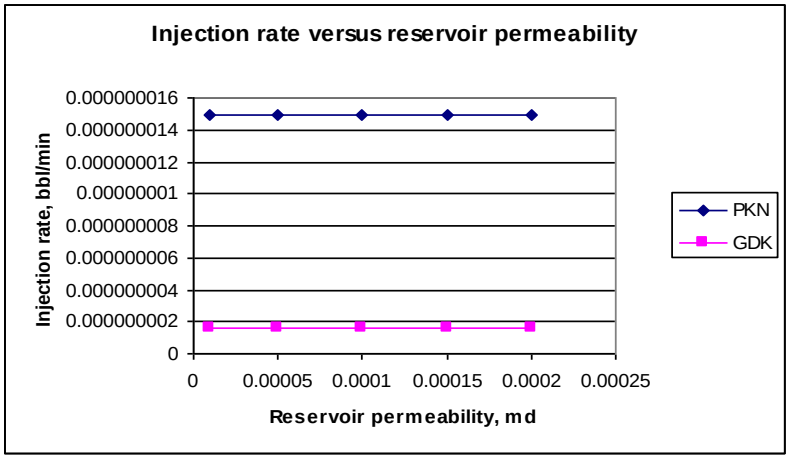

Figure 52- Design study using Case 1 for PKN and GDK models on required injection rate against reservoir permeability.

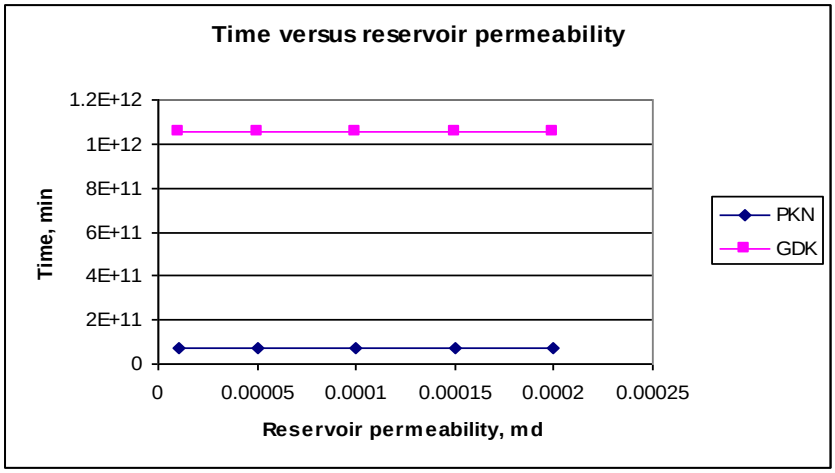

Figure 53 Design study using Case 1 for PKN and GDK models on required time against reservoir permeability.

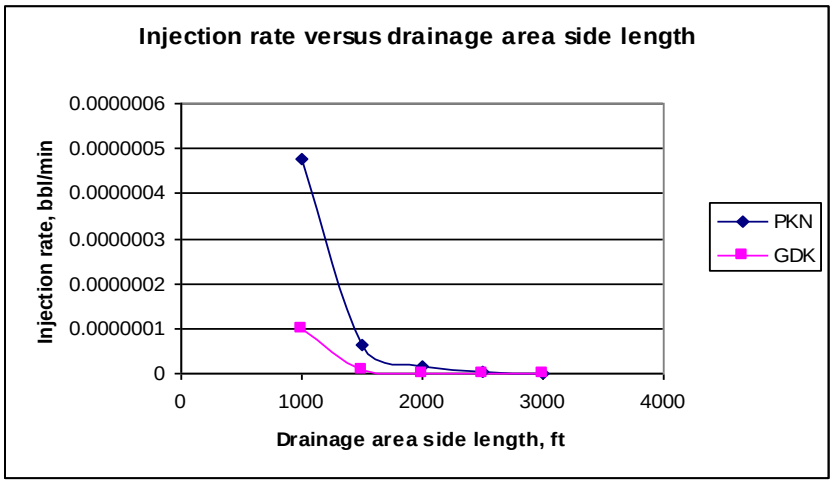

Figure 54- Design study using Case 1 for PKN and GDK models on required injection rate against drainage area side length.

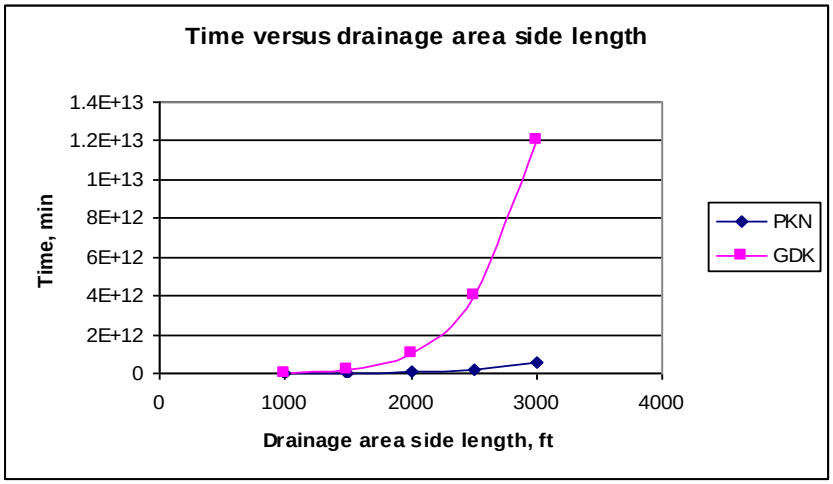

Figure 55- Design study using Case 1 for PKN and GDK models on required time against drainage area side length.

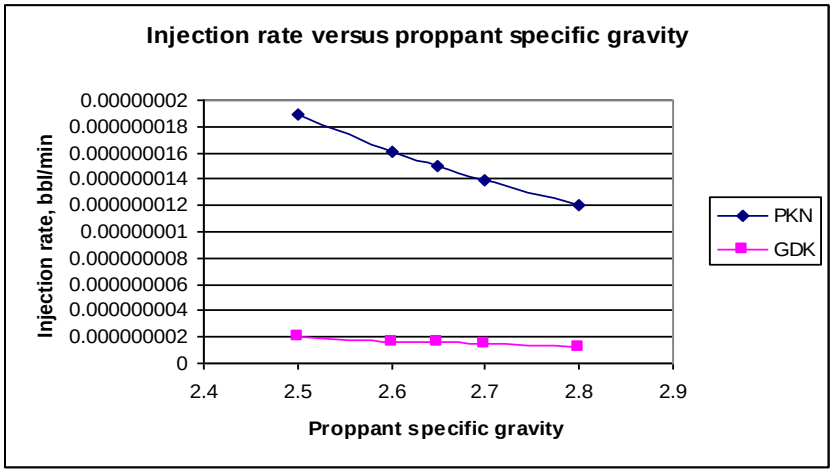

Figure 56- Design study using Case 1 for PKN and GDK models on required injection rate against proppant specific gravity.

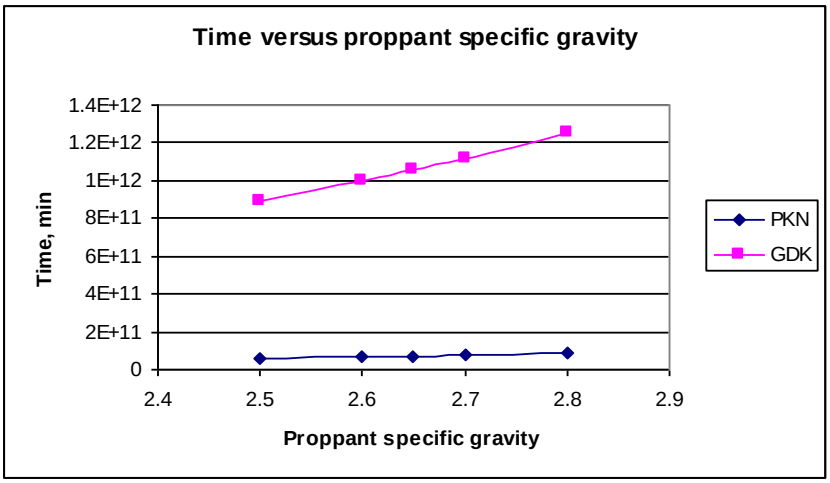

Figure 57- Design study using Case 1 for PKN and GDK models on required time against proppant specific gravity.

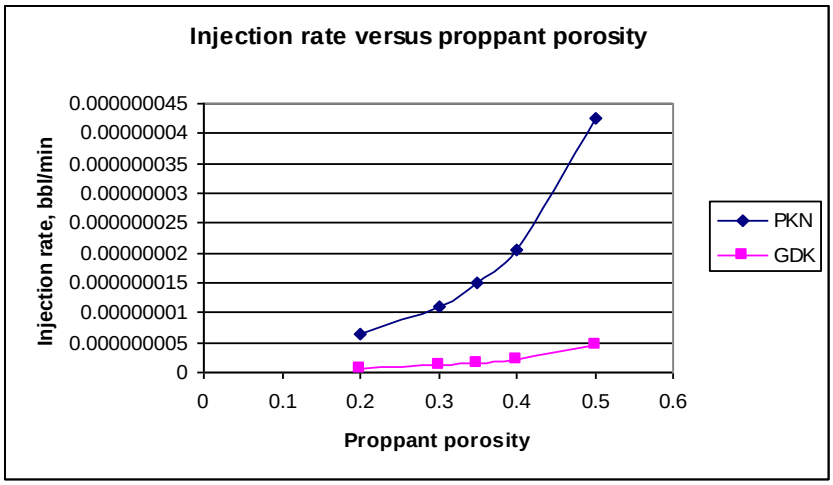

Figure 58- Design study using Case 1 for PKN and GDK models on required injection rate against proppant porosity.

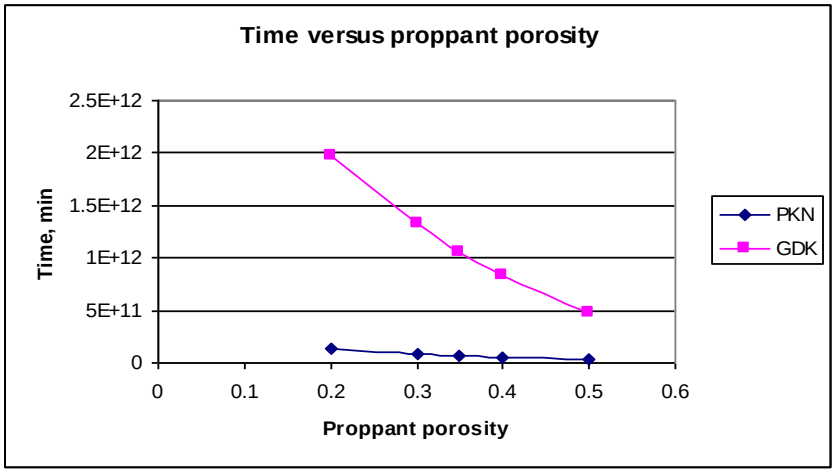

Figure 59- Design study using Case 1 for PKN and GDK models on required time against proppant porosity.

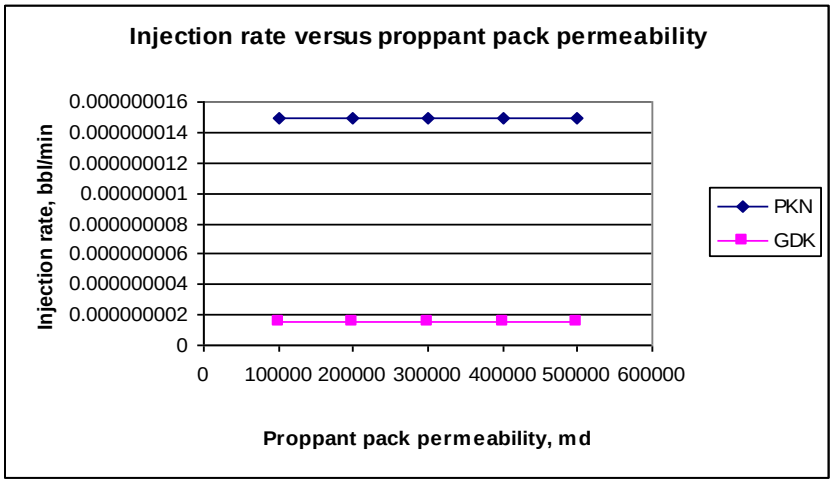

Figure 60- Design study using Case 1 for PKN and GDK models on required injection rate against proppant pack permeability.

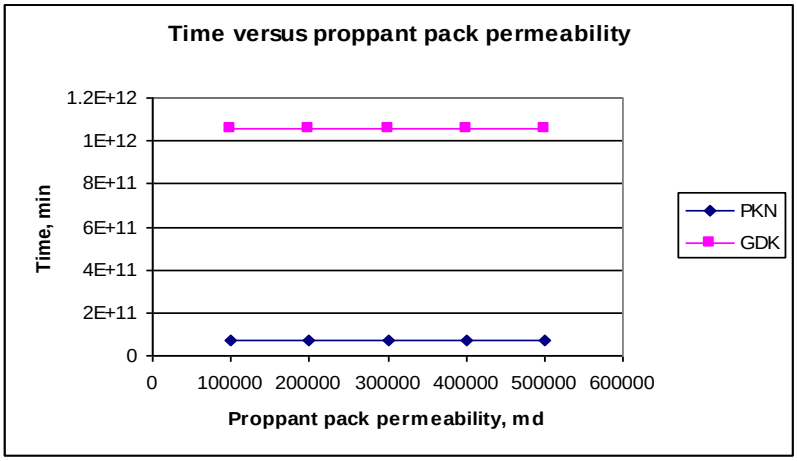

Figure 61- Design study using Case 1 for PKN and GDK models on required time against proppant pack permeability.

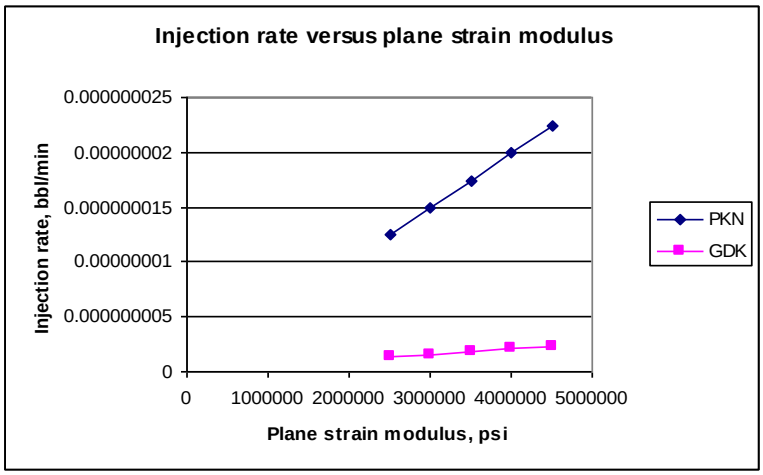

Figure 62- Design study using Case 1 for PKN and GDK models on required injection rate against plane strain modulus.

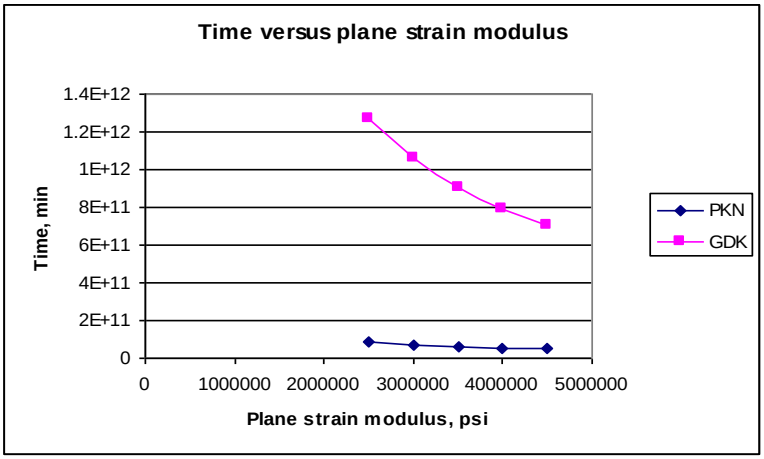

Figure 63- Design study using Case 1 for PKN and GDK models on required time against plane strain modulus.

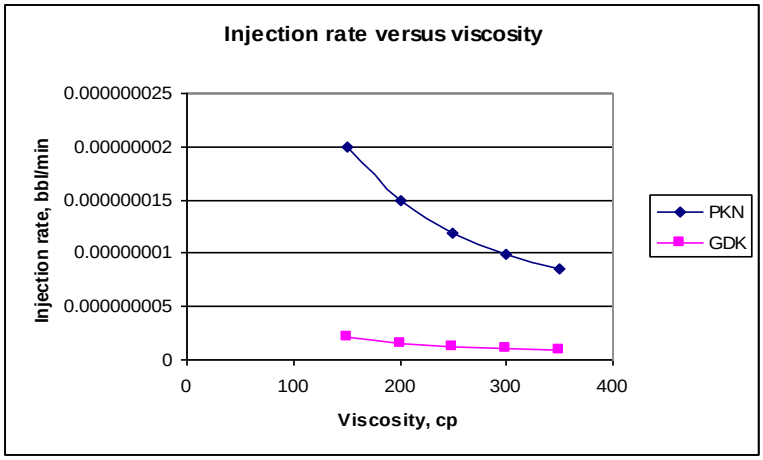

Figure 64- Design study using Case 1 for PKN and GDK models on required injection rate against viscosity.

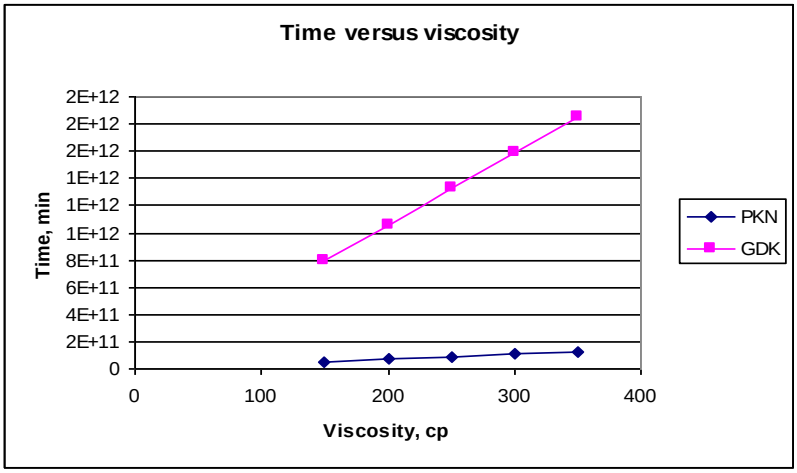

Figure 65- Design study using Case 1 for PKN and GDK models on required time against viscosity.

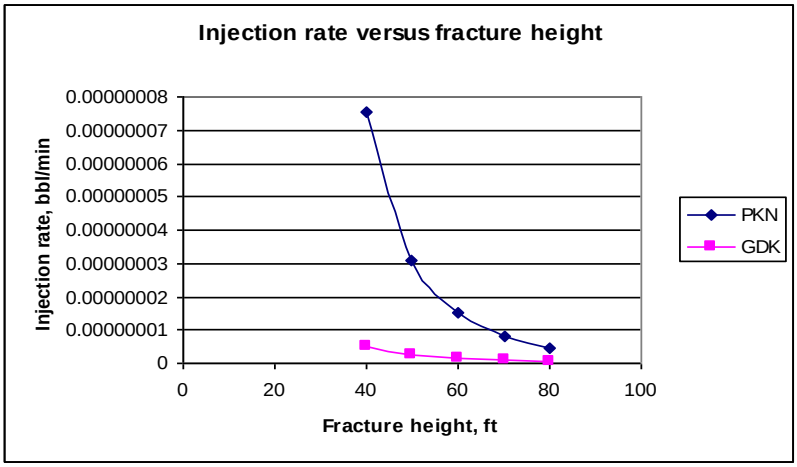

Figure 66- Design study using Case 1 for PKN and GDK models on required injection rate against fracture height.

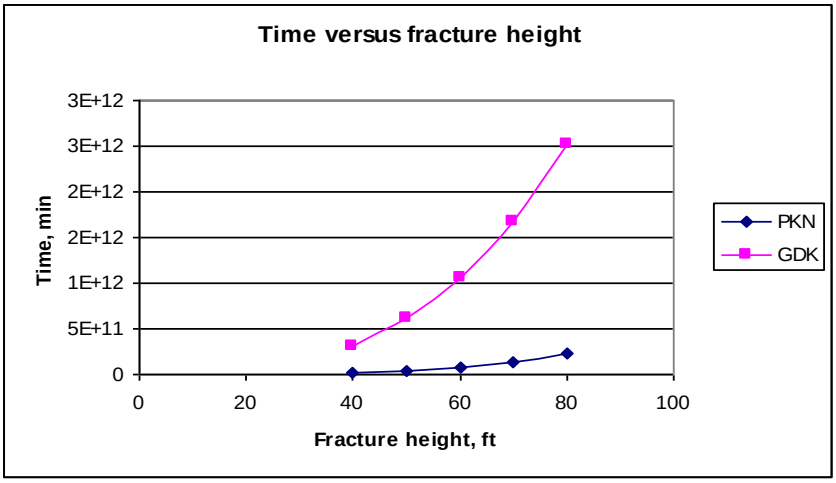

Figure 67- Design study using Case 1 for PKN and GDK models on required time against fracture height.

Appendix F: Design Study PKN Model Case 2 Results

Table 22- Results for design study sensitivity analysis using PKN Model Case 2 for parameters proppant mass, reservoir permeability, drainage area side length, proppant specific gravity and proppant porosity.

		PKN model Case 2	
Parameter	**Value**	**Injection rate, bbl/min**	**Time, min**
Proppant mass, lbm	100000	1.04E-09	3.27E+24
	200000	1.67E-08	1.28E+22
	300000	8.45E-08	4.99E+20
	400000	2.67E-07	4.99E+19
	500000	6.52E-07	8.37E+18
Reservoir permeability, md	0.00001	1.67E-08	1.28E+22
	0.00005	1.67E-08	1.28E+22
	0.00010	1.67E-08	1.28E+22
	0.00015	1.67E-08	1.28E+22
	0.00020	1.67E-08	1.28E+22
Drainage area side length, ft	1000	5.34E-07	3.12E+18
	1500	7.03E-08	4.05E+20
	2000	1.67E-08	1.28E+22
	2500	5.47E-09	1.86E+23
	3000	2.20E-09	1.66E+24
Proppant specific gravity	2.50	2.11E-08	8.02E+21
	2.60	1.80E-08	1.10E+22
	2.65	1.67E-08	1.28E+22
	2.70	1.55E-08	1.48E+22
	2.80	1.34E-08	1.98E+22
Proppant porosity	0.20	7.27E-09	6.73E+22
	0.30	1.24E-08	2.31E+22
	0.35	1.67E-08	1.28E+22
	0.40	2.30E-08	6.74E+21
	0.50	4.76E-08	1.57E+21

Table 23- Results for design study sensitivity analysis using PKN Model Case 2 for parameters proppant pack permeability, plane strain modulus, viscosity, fracture height and aspect ratio.

		PKN model Case 2	
Parameter	**Value**	**Injection rate, bbl/min**	**Time, min**
Proppant pack permeability, md	100000	1.67E-08	1.28E+22
	200000	1.67E-08	1.28E+22
	300000	1.67E-08	1.28E+22
	400000	1.67E-08	1.28E+22
	500000	1.67E-08	1.28E+22
Plane strain modulus, psi	2500000	1.39E-08	1.84E+22
	3000000	1.67E-08	1.28E+22
	3500000	1.95E-08	9.39E+21
	4000000	2.22E-08	7.19E+21
	4500000	2.50E-08	5.68E+21
Viscosity, cp	150	2.22E-08	7.19E+21
	200	1.67E-08	1.28E+22
	250	1.33E-08	2.00E+22
	300	1.11E-08	2.87E+22
	350	9.53E-09	3.91E+22
Fracture height, ft	40	8.45E-08	2.22E+20
	50	3.46E-08	2.06E+21
	60	1.67E-08	1.28E+22
	70	9.00E-09	5.97E+22
	80	5.28E-09	2.27E+23
Aspect ratio	0.10	1.67E-08	1.28E+22
	1.00	1.67E-08	1.28E+22
	0.01	1.67E-08	1.28E+22